Sustainable Cities and Society 136 (2026) 107084

Contents lists available at ScienceDirect

Sustainable Cities and Society

journal homepage: www.elsevier.com/locate/scs

How much do users matter? An integrated method for building flood vulnerability and exposure assessment in Historic Urban Areas

Gessica Sparvoli [a], Elena Bosi [b], Gabriele Bernardini [*,a], Enrico Quagliarini [a], Tiago Miguel Ferreira [c]

[a] DICEA, Università Politecnica delle Marche, via brecce bianche 12, 60131 Ancona, Italy
[b] DAStU, Politecnico di Milano, via Bonardi, 3, 20133 Milan, Italy
[c] CERIS, Instituto Superior Técnico, University of Lisbon, Av. Rovisco Pais 1049-001, Lisboa, Portugal

ARTICLE INFO

Keywords:
Historic urban areas
Flood risk
User exposure
User vulnerability
Spatiotemporal analysis

ABSTRACT

The definition of sustainable strategies for risk mitigation in Urban Built Environments (UBEs) prone to flooding should be based on holistic yet quick approaches that comprise hazard, physical vulnerability, and user factors. In particular, the ways users occupy, live and behave in UBEs introduce significant spatiotemporal dynamics in the final risk due to their user exposure (how many?) and vulnerability (of which type?). These effects can be relevant in Historic UBEs (HUBEs), due to building heritage features and the related need to balance mitigation strategies with conservation and preservation. Therefore, quickly applicable analyses, exploiting available databases, should be developed, and the reliability of methods that incorporate user-related, dynamic parameters should be demonstrated in comparison to established "static" analyses of hazards and physical elements. This work proposes a building-scale approach for vulnerability and exposure assessment to floods, aimed at identifying "hot-spots" in HUBEs, by combining "static" and "dynamic" assessment methods. "Static" (e.g. material degradation, construction typology, urban morphological features) and "dynamic" (e.g. daily occupancy schedules, occupant densities/typologies) are combined within a GIS database, using single and multi-factor metrics. The method is demonstrated using a relevant Italian case study. Results remark that considering user exposure and vulnerability over time introduces significant differences in flood risk metrics and HUBEs hotspots, for both public buildings, due to daytime occupancy schedules, and residential buildings, where risk levels increase up to 80%, considering the possible low physical vulnerability of these buildings. This work therefore provides robust approaches to support informed decision-making in the prioritisation of targeted mitigation strategies within HUBEs.

1. Introduction

In recent years, the increasing frequency, intensity and socio-economic impacts of flood events, driven by climate change, urban expansion, and land-use transformations, have significantly exacerbated both exposure and vulnerability of urban areas worldwide (Bernardini et al., 2021; da Silva et al., 2022). In fact, floods represent one of the most damaging and recurring natural hazards, causing casualties, displacements and long-term disruptions to urban infrastructures, services and heritage assets (Arrighi et al., 2023; Vojinovic et al., 2016). The intensification of extreme rainfall, storm surges, and riverine overflows has produced increasingly frequent and unpredictable inundation dynamics, which challenge conventional design and management thresholds (Kim et al., 2024; Zhao et al., 2023). Flood affecting urban areas manifests in different forms, including riverine, pluvial, coastal, or flash floods, depending on specific hydrological and geomorphological factors. These events are commonly evaluated in probabilistic terms, such as 50- or 100-year return periods (Ferreira & Santos, 2020), to guide infrastructure planning and risk communication. Despite improved flood governance and planning frameworks (e.g. EU Floods Directive, 2007/60/EC, 2007; ISPRA, 2025), the flood risk remains significant. Main causes are related to structural, regulation and financial constraints, including the inadequate maintenance of drainage infrastructure, insufficient urban planning integration, and limited adaptability in heritage or densely built areas (Arrighi et al., 2018; Bernardini et al., 2025).

* Corresponding author.
E-mail address: g.bernardini@staff.univpm.it (G. Bernardini).

https://doi.org/10.1016/j.scs.2025.107084
Received 23 July 2025; Received in revised form 16 December 2025; Accepted 17 December 2025
Available online 17 December 2025

Among the most critically affected contexts, Historic Urban Built Environments (HUBEs) are particularly relevant, prone to significant risk levels due to the overlapping and combination of different conditions, in view of the interactions between components from their Social, Ecological, and Technological Systems (SETS) (Sharifi, 2023). The technological system comprises the physical components of the built environment, from buildings to urban design and form, and its infrastructure, thus being also affected by conservation and preservation constraints, which can limit structural interventions for risk mitigation (Arrighi et al., 2018; Kim et al., 2024; Lassandro et al., 2024; Wang, 2015). These issues are hence associated with the intrinsic features characterising the physical vulnerability and exposure, or even susceptibility, of HUBEs and their composing elements, starting from its single buildings, streets and urban squares (Agliata et al., 2021; Davis et al., 2023; Mebarki et al., 2012; Romão et al., 2016; Stephenson & D'Ayala, 2014). The ecological system mainly concerns the environment and climatic conditions, along with land use. HUBEs are often located in geomorphologically sensitive areas, such as river floodplains or coastal, and are characterised by their inherent structural and functional fragilities, due to their dense, stratified urban fabrics and a built heritage associated with high architectural, historical, cultural, and symbolic values (Arrighi et al., 2018; Bernardini et al., 2025; Miranda & Ferreira, 2019; Zhao et al., 2023). Finally, the social system relates to the users, as individuals and community as a whole. In this sense, HUBEs are also affected by a complex system of socio-economic functions, characterised by a possible high variability in the number and typologies of hosted users (Bernabeu-Bautista et al., 2023; Bernardini et al., 2024; MILEU & QUEIRÓS, 2022; Zakariya et al., 2014). Occupancy schedules can vary daily/weekly, exacerbated by tourist flows correlated with the HUBE tangible and intangible heritage, as well as by the presence of vulnerable users, such as elderly, children, and users with reduced mobility, who are often present in historic residential buildings and public or healthcare facilities within HUBEs, and could need specific assistance in case of a flood emergency (Hsiao et al., 2021). This led to additional complexities in the interactions between heritage conservation requirements and the need to ensure safety and resilience, thus supporting the development of reliable rules for the "dynamic" assessment of user exposure and vulnerability (Holicky & Sykora, 2010; Vojinovic et al., 2016).

In view of the above, moving towards effective flood risk reduction and mitigation in HUBEs requires the availability of assessment methodologies that explicitly consider both the physical characteristics of the built environment and the "dynamic" variability of user presence. Mapping risk at the proper spatial and temporal scale and prioritising interventions according to realistic scenarios are critical for effective, context-sensitive strategies, with explicit attention to the interactions among SETS dimensions and components (Sharifi, 2023). Moreover, a microscale approach, focused on the building scale, could support such assessment tasks considering the basic physical elements also associated with use dynamics depending on hosted functions, and with fundamental components in shelter-in-place strategies and vertical evacuation (Kim et al., 2024; Lumbroso & Davison, 2018).

To address these challenges, this work proposes a novel and refined operational methodology providing for integrated flood vulnerability and exposure assessment, by excluding the components of flood hazard and focusing on:

- "static" analysis on the HUBE intrinsic physical building components (Agliata et al., 2021), starting from validated methods for building Physical Vulnerability (PV) assessment (Ferreira & Santos, 2020).
- "dynamic" analysis on User-related components, which integrates spatiotemporal human activity patterns and socio-demographic attributes (Bernardini et al., 2020; H. Chen et al., 2022). This assessment builds on previous methods for User Exposure and Vulnerability (UEV) assessment at urban and mesoscale levels, adapting them to focus on the microscale to enhance correlation with building occupancy patterns (Miranda & Ferreira, 2019; Quagliarini et al., 2023).

A Geographic Information System (GIS) environment (Y. Chen, 2022; da Silva et al., 2020) is used to ensure consistent data collection and analysis. The relevance of "static" and "dynamic" components is then quantified through the Analytic Hierarchy Process (AHP), selected as a consolidated technique in flood vulnerability, exposure, risk and mitigation strategies evaluations (Agliata et al., 2022; Ashfaq et al., 2025; Huang & Feng, 2025; Malekinezhad et al., 2021; Pacetti et al., 2022; Papathoma-Köhle, 2016). Then, differences in building-scale outputs considering only PV and the combination of PV and UEV into an integrated Exposure and Vulnerability Index are also evaluated to trace the importance of including user factors in the assessment process.

In this way, the novelty and distinct contribution of this study lie in two main aspects:

1. The methodological separation of vulnerability and exposure assessment from hazard assessment generates a flexible, hazard-independent framework adaptable to evolving multi-hazard flood contexts and facilitating broader multi-risk applications. This approach enables a consistent evaluation of intrinsic physical and social components, regardless of specific flood hazard types or intensities. This innovation is complemented by the development of a novel operational workflow that balances methodological rigour with practical applicability, overcoming common limitations of traditional flood risk assessments that rely largely on "static", hazard-specific indicators;
2. The systematic integration and empirical validation of spatiotemporal user dynamics, performed at the building scale within HUBEs, reveal how temporal occupancy variations and social vulnerability interact with structural fragility to modulate overall vulnerability levels. This refined approach advances beyond traditional "static" assessments by providing actionable insights for targeted preparedness and mitigation strategies in complex urban heritage environments.

The method is tested in the historic centre of Bagnacavallo (Ravenna, Italy), a representative heritage site within the floodplain of the Po Valley, whose territory has been recently affected by devastating floods (Carminati & Martinelli, 2002; Castaldini et al., 2019; ISPRA, 2025). The case study demonstrates the applicability of the framework in a real-world heritage context, providing empirical evidence of how user dynamics can be operationally integrated into vulnerability and exposure assessments.

2. Literature review

HUBEs represent critical scenarios in which overall flood risk levels are widely affected by the combination of physical features, functional and social dimensions, and constraints posed by the built environment, urban morphology and its functions (Davis et al., 2023; Julià & Ferreira, 2021; Pacetti et al., 2022). Preservation, conservation and local heritage identity criteria often present constraints that limit structural adaptation measures, such as physical interventions on buildings and infrastructures (Arrighi et al., 2018; Kim et al., 2024; Lassandro et al., 2024; Wang, 2015). Consequently, non-structural measures, including emergency planning and risk communication, must be carefully tailored to the specific risk scenarios that may arise (La Rosa & Pappalardo, 2020; Lumbroso & Davison, 2018; Musolino et al., 2022).

To support such issues, flood risk assessment methodologies have currently been conducted at the *meso* or macro scale (e.g., city or district levels), with the aim of prioritising interventions for broader urban systems (Vojinovic et al., 2016; Young & Jorge Papini, 2020). However, recent literature increasingly emphasises the need for a shift in scale, moving from urban or district-level assessments to more detailed

micro-scale analyses, specifically at the level of individual buildings (Bernardini et al., 2021; Kim et al., 2024). In fact, this scale can collect many relevant parameters for flood risk, associated with both physical components and user-related factors, and thus on their vulnerability and exposure.

Previous works provided a structured analysis of parameters affecting intrinsic physical vulnerability and exposure (or even susceptibility) of buildings (Agliata et al., 2021). Assessment methods can take advantage of index-based methods, well-suited to contexts where the objective is to characterise the intrinsic fragilities of buildings through a multicriteria analysis, rather than to model deterministic hazard scenarios (Miranda & Ferreira, 2019). Composite index-based assessments also make it possible to integrate different dimensions of vulnerability and exposure within a single framework, producing clear and interpretable outputs that can support both researchers and decision-makers (Davis et al., 2023). Existing approaches also typically combine flood hazard characteristics (e.g., water depth, velocity and extent) with physical features of the built environment, such as the conservation state, building typology (type of resisting system), number of floors, and the presence and dimension of openings (Julià & Ferreira, 2021). These methods offer robust and scalable frameworks, particularly effective for prioritising interventions at the city or district scale. Nevertheless, the need for incorporating additional categories of parameters related to the buildings but expressing factors on social vulnerability has also been remarked, promoting the first step towards loss or damage assessment (Agliata et al., 2021). In fact, consolidated methods seem to inherently overlook the role of human presence on risk, failing to account for how user occupancy, typology, and spatiotemporal variations influence the actual risk, which can have larger impacts especially in HUBEs, due to the combination with their intrinsic physical features (Bernardini et al., 2024).

To overcome these limits, efforts to manage additional building parameters have been performed. In particular, the number of floors is a relevant indicator to derive information about the potential number of occupants (mainly, residents) or the potential availability of sheltering associated with vertical evacuation procedures (Agliata et al., 2021; Papathoma-Köhle, 2016; Papathoma-Köhle et al., 2011). Moreover, buildings are characterised by different occupancy schedules, opening times and operating hours, and are hence associated with varying daily occupancy patterns and population distribution, especially in public functions (Bernardini et al., 2020, 2024; H. Chen et al., 2022; Cherfaoui & Djelal, 2019; MILEU & QUEIRÓS, 2022; Zakariya et al., 2014). In HUBEs with high touristic relevance, seasonal fluctuations further influence user exposure and vulnerability. Peak tourism periods bring substantial temporary increases in population density, which can intensify flood risks and strain emergency response capabilities (Camacho-Caballero et al., 2025; Jaafari et al., 2024; Musolino et al., 2022; Renner et al., 2018). Hence, incorporating "dynamic", user-related parameters into flood risk assessments is essential for capturing the temporal variability of risk and for supporting effective, context-sensitive mitigation strategies capable of addressing the limitations of "static", physical-based models (da Silva et al., 2020; Ferreira & Santos, 2020; Mebarki et al., 2012; Miranda & Ferreira, 2019).

In this sense, a growing body of research has started to highlight that flood risk in HUBEs is strongly influenced by user-related dynamics, including the patterns of use, accessibility, spatiotemporal distribution of users, their familiarity with the environment, and their ability to activate and follow emergency protocols (Bernardini et al., 2021, 2024; H. Chen et al., 2022; da Silva et al., 2022). These aspects are particularly relevant in a historic context where multiple building uses – residential, commercial, institutional and cultural – interact through complex daily and seasonal dynamics. Socio-demographic characteristics further impact vulnerability (Bernardini et al., 2020, 2024; Mileu & Queirós, 2022; Quagliarini et al., 2023): elderly, toddlers and generally individuals with reduced mobility often require more time or support to evacuate and may be less capable of responding effectively to emergency alerts. These groups are frequently present in historic residential buildings or may be comprised within transient users of public and healthcare facilities, thereby increasing the functional vulnerability of specific structures. This kind of approach has also been explored in studies of other sudden-onset disasters (Dabbeek et al., 2025; Jaafari et al., 2024).

Despite a growing interest in resilience-building for historic areas, the integration of user-related factors into flood risk assessments remains limited (Bernardini et al., 2021, 2024; Quagliarini et al., 2023). Most existing methods are typically limited to aggregated urban scales or focus primarily on open spaces, evacuation routes, and public facilities (D'Amico et al., 2023; Renner et al., 2018), with limited attention to building-scale vulnerabilities and their interactions with HUBEs' complex urban fabric.

Recent studies, therefore, call for context-sensitive, local-scale approaches capable of capturing the variable and evolving nature of vulnerability in HUBEs (da Silva et al., 2022; Kim et al., 2024; Renner et al., 2018). This gap highlights the need for adaptive, data-efficient frameworks that balance physical vulnerability with "dynamic", user-related functional dimensions in HUBEs. While "static" physical assessments provide a solid baseline, incorporating "dynamic", human-centred analyses significantly improve flood risk characterisation by revealing different scenarios based on complex interactions among urban form, building function and occupant patterns. Our study contributes to this research by providing a practical framework for quantifying these effects at the building scale, while still referring to the exposure and vulnerability components of risks. Therefore, the proposed approach is applicable as a valuable reference to collect these intrinsic risk scenario inputs, to be then potentially applied in multiple flood hazard conditions.

3. Case study: the historic centre of bagnacavallo

The Historic Centre of Bagnacavallo, located in the province of Ravenna (Emilia-Romagna, Italy), represents a characteristic example of a medieval urban settlement in the Po Valley, Italy's largest floodplain. The area is intrinsically prone to flooding due to its geomorphological nature as an alluvial plain, yet it has long been attractive for settlement due to its flat terrain and proximity to watercourses.

The Flood Risk Management Plan (FRMP) is the official tool introduced in Italy to provide an overall framework for assessing flood risk, in line with the European Floods Directive (Directive 2007/60/EC on the assessment and management of flood risks). FRMPs in Italy are coordinated at the River Basin District or at the regional level, and they include flood hazard and risk maps for areas identified as being potentially at significant risk. The designation of such areas is grounded on records of historical floods. According to the Flood Risk Management Plan of Emilia-Romagna region (Piano di Gestione del Rischio da Alluvione - PGRA), the entire Historic Urban Built Environment (HUBE) of Bagnacavallo is considered to be potentially exposed to medium flood risk scenarios, as shown in Fig. 1. Similar conclusions are drawn in the local Civil Protection Emergency Plan (Piano di Emergenza e di Protezione Civile, last accessed October 17, 2025), which confirms a moderate hazard for the area but a high-risk level, when also considering factors such as urban density and the historic value of the built environment.

Moreover, the town of Bagnacavallo was affected by the massive 2023 Emilia-Romagna flood, as documented in the flood extent maps produced by the Emilia-Romagna region (Perimetrazione aree allagate eventi 2023-2024) during the emergency phase, as well as in the local Civil Protection interactive map (WebSIT, last accessed October 17, 2025) showing flooded areas from 1996 to 2024. These maps show that while the HUBE itself was not directly affected, flooded areas extended all around the town's historic core. This nevertheless makes Bagnacavallo's HUBE highly relevant for analysis, given the probability of future floods combined with the high cultural value of its built heritage.

The town originated during the early Middle Ages along a meander

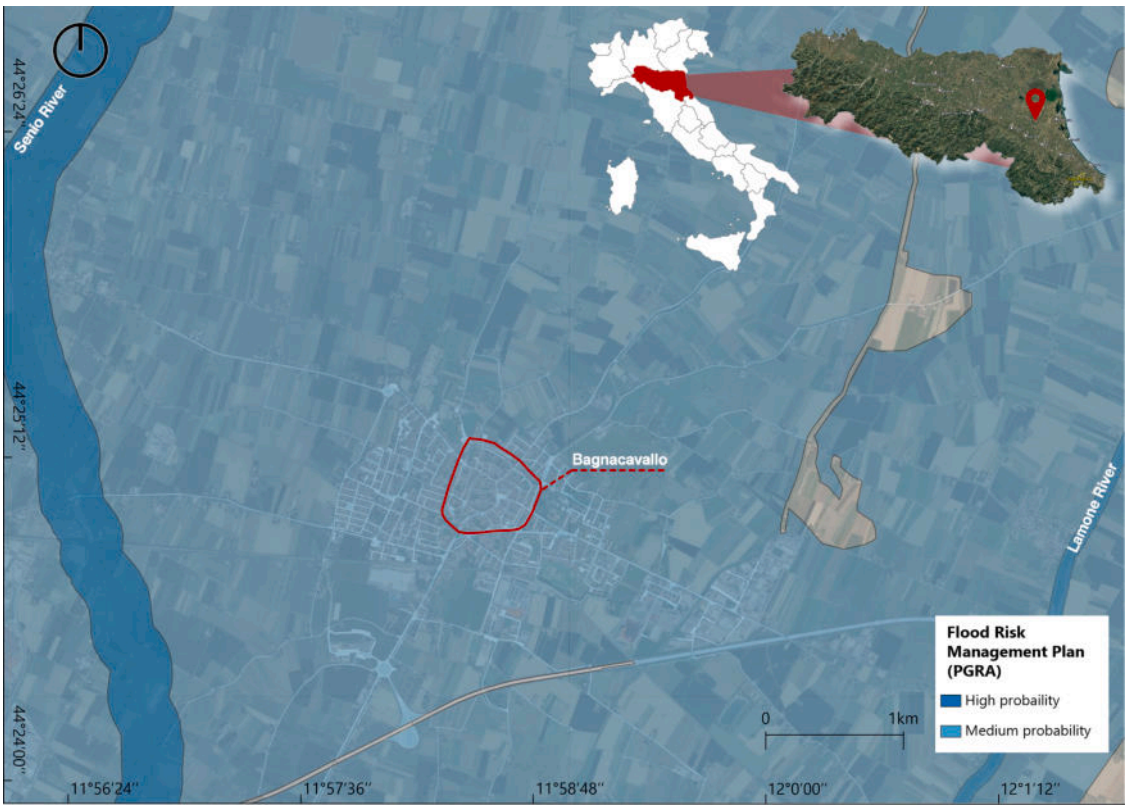

Fig. 1. Overview of the historic city centre of Bagnacavallo (Ravenna, Italy – general position in the region on the upper right corner) with respect to the proximity to watercourses (Senio and Lamone Rivers) and to flood risk probability levels under different hazard scenarios (Perimetrazione aree allagate eventi 2023-2024). The HUBE considered in this work is marked by the red boundary.

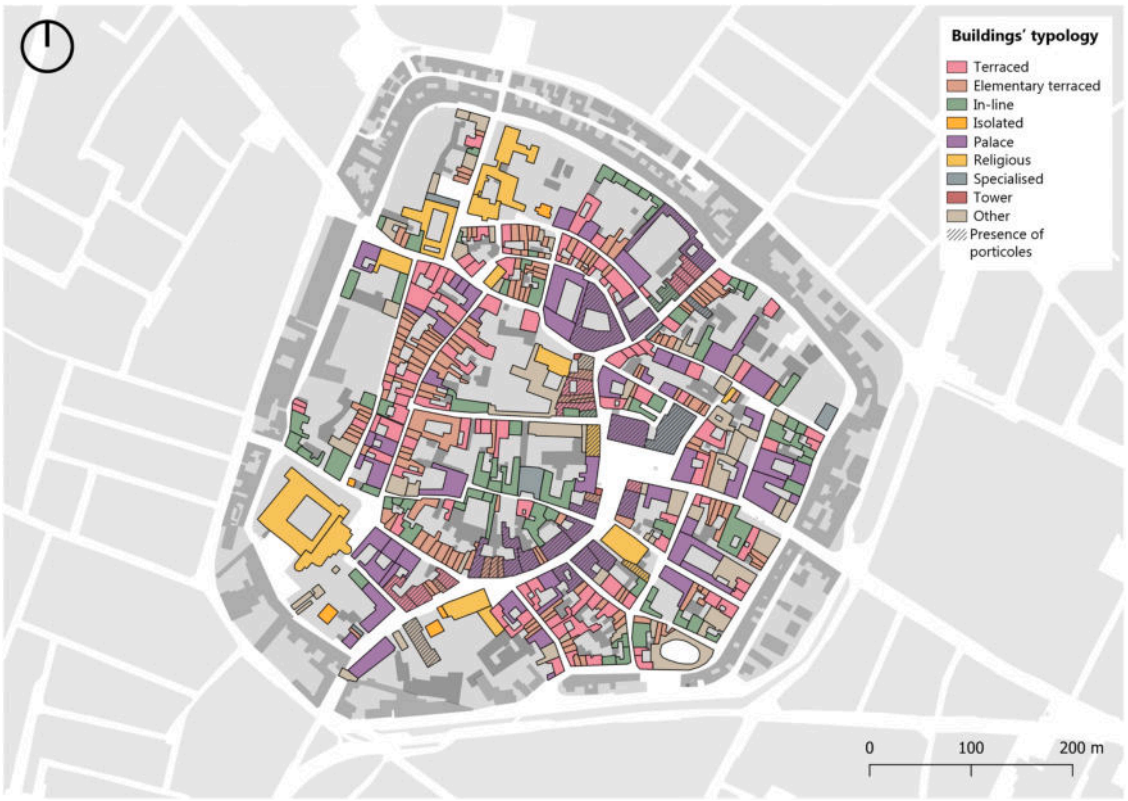

Fig. 2. Map of the buildings' typology.

of the Senio River, with a fortified core (citadel) and external market space, reflecting typical defensive and economic layouts of Lombard-era settlements. Although the river's course has shifted or disappeared over time due to reclamation efforts, its historical influence remains evident in Bagnacavallo's urban morphology, particularly in the alignment of the main road (Via Maestra) and public squares (Calbi, A.; Susini, 1994).

The main historic area of Bagnacavallo includes approximately 700 buildings, with this study focusing on 468 buildings from the innermost, representing the pre-19th-century portion. This area is characterised by high building density, porticoes along the streets, traditional masonry construction, and distinct aggregation patterns, and thus it is representative of many other towns across the Emilia Romagna Region, and in particular of the Po Valley (Cantatore, 2023; Montanari, M.; Ridolfi, M.; Zangheri, 2004). In this sense, as shown in Fig. 2, the main building typologies are presented in Bagnacavallo and other similar HUBEs, including:

- Elementary Terraced Houses, some dating back to the 14th century Row Houses, prevalent in the southeast, with irregular additions.
- Bourgeois Houses, formed by aggregating smaller units.
- Palaces, with extensive façades (often modified with porticoes) and inner courtyards, more vulnerable due to their openness and location on wider streets.

The following data collection strategy (Section 4.1) outlines the sources and methods used to obtain building information.

4. Methodology

The work is composed of four main phases, as shown in the workflow presented in Fig. 3. The first phase concerns the collection, organisation, and integration of the data within GIS tools (Section 4.1), to provide the analytical basis for the following phases. The second phase involves assessing the physical vulnerability of the buildings and their exposure to flooding events (Section 4.2). The third phase addresses the evaluation of user exposure and vulnerability (Section 4.3). In both the second and third phases, consolidated and validated methods have been adopted and innovatively integrated by adding relevant parameters. Non-dimensional, normalised indices are also defined to allow all specific results to range from 0 (generally excluded) to 1 (as the maximum, and thus critical, value). Finally, the last phase integrates the PV and UEV components through the proposed Integrated Vulnerability and Exposure Index (IVE) and its differential form (dIVE), enabling the analysis of their combined and relative influence on overall vulnerability patterns at the building scale within the HUBE (Section 4.4).

4.1. Data collection and management processes and integration into GIS tools

The data collection and management processes were developed to support a systematic and transparent building-scale assessment. This involved the acquisition, organisation, and integration of spatial and descriptive information into a GIS-based analytical framework. The input dataset includes two main groups of parameters, detailed further in Sections 4.2 and 4.3. The first group includes physical and morphological building attributes, such as construction material, number of floors, façade and opening configuration, presence of basements, and threshold height. These characteristics describe the structural, geometric and conservation-related features of each building and are required to assess physical vulnerability. The second group concerns functional and occupancy-related attributes, including the intended use of each building, floor-based distribution of functions, operating schedules and corresponding occupancy levels. These characteristics define how buildings are used and populated over time and are essential for assessing exposure and social vulnerability.

The adoption of a GIS environment provides several advantages for assessing the considered microscale in flood contexts (Ashfaq et al., 2025; da Silva et al., 2020). It enables spatially explicit representation and analysis, allowing the identification of spatial patterns, clustering of vulnerabilities, and location-specific risk hot-spots. It supports the integration of heterogeneous datasets (e.g., cadastral, infrastructural, demographic) into a unified analytical framework, enhancing data consistency and redundancy. Furthermore, GIS enables scalable and reproducible workflows, essential for updating analyses as new data

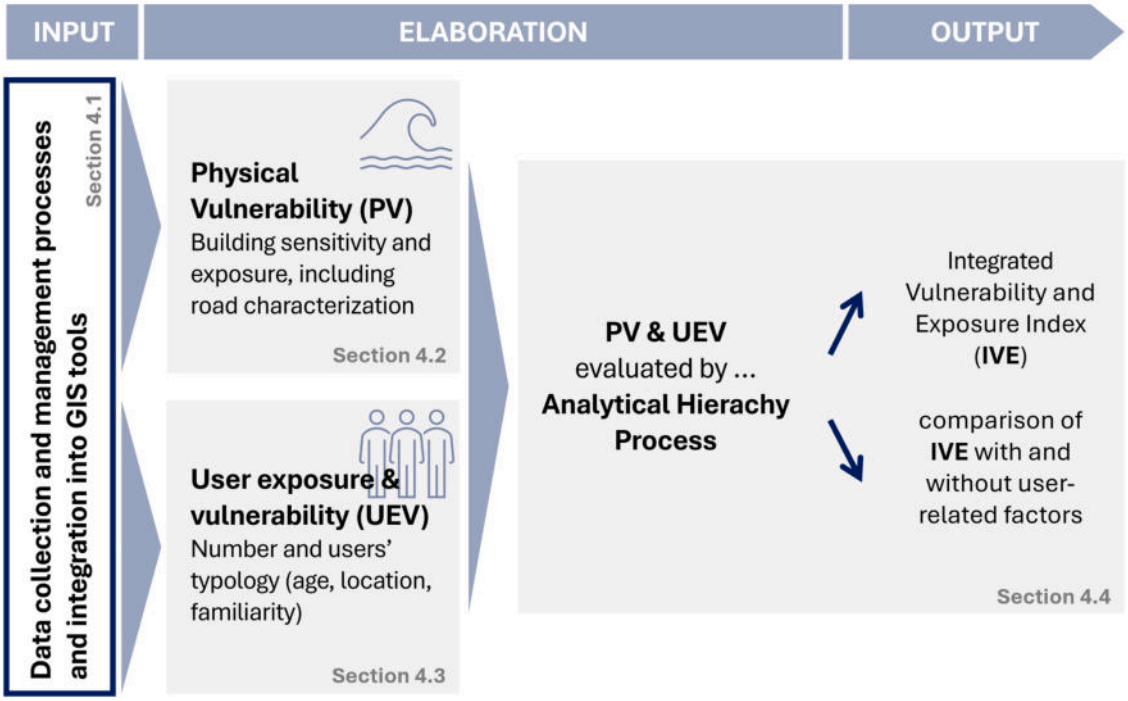

Fig. 3. Workflow of the methodological steps for each phase of the study, including the reference to the specific sub-sections in which each of them is described.

become available or when assessing other urban areas with similar methods. The GIS environment also facilitates visualisation tools that are highly valuable for communicating risk-related information to decision-makers, stakeholders, and the public, thereby supporting informed spatial planning, targeted mitigation strategies, and improved emergency preparedness.

All datasets used in the GIS environment were derived from open-access and institutional repositories to ensure transparency, comparability, and replicability across different HUBEs. Building footprints, road networks, and city blocks were obtained as shapefiles from the Emilia-Romagna regional mapping service (Geoportale - Regione Emilia Romagna) and from municipal open data portals. Detailed building-scale information, including construction materials, number of stories, construction year, and conservation status, was obtained from the municipality's Historic Centre Survey Plan (Piano Particolareggiato del Centro Storico - PPCS 2023, last accessed October 17, 2025), which provides systematic on-site survey data available across most regional municipalities. Open platforms such as Google Maps and Google Street View were also used to verify and complement data on structural and morphological characteristics (Kang et al., 2018; Li et al., 2025).

The same survey dataset supported social vulnerability and exposure assessments (Section 4.3). Based on these data, nine different use categories were identified across the 468 buildings analysed. As shown in Fig. 4, the spatial distribution of these functions reflects the historic development and the socio-economic organisation of the area, serving as a basis for estimating user presence and functional occupancy patterns. This provides a consistent and easy-to-apply floor-based modelling approach, practical for implementation by local administrations and technical offices using standard GIS data.

Social vulnerability was further evaluated through the analysis of the demographic composition of the local population, utilising the latest available data at the municipal level. For the Italian case study, this information was retrieved from the 2024 national census, published by the Italian National Institute of Statistics (ISTAT). The dataset provides detailed age distributions, enabling comprehensive demographic characterisation of the study area.

The collected information was systematically compiled and managed into a GIS-based database using QGIS (QGIS). This integration of "static" morphological building features with "dynamic" use attributes forms the foundation for detailed vulnerability analysis and exposure assessment.

Hazard data were intentionally excluded at this stage to focus on intrinsic vulnerability and exposure independently of hazard-specific scenarios. Nevertheless, the case study area is classified as high flood-risk by national and regional planning instruments, ensuring contextual relevance and allowing future integration with empirical or modelled flood data.

To ensure applicability across different data availability scenarios, the method relies on standardised typology classes, degradation scales, and occupancy load factors. These elements facilitate systematic application and reproducibility across multiple HUBEs. Temporal dynamics were captured through four representative daily intervals: morning (8:00–13:00), afternoon (14:00–19:00), evening (20:00–01:00), and night (02:00–07:00). These intervals are defined according to typical patterns of user behaviour and the opening hours of buildings and public spaces within the study area. Integrating this temporal dimension enables "dynamic" modelling of daily variations in space utilisation, enhancing the realism, accuracy and relevance of vulnerability and risk evaluations, particularly in complex and historically layered urban contexts.

4.2. *Physical vulnerability assessment and exposure to flooding*

In this study, the physical vulnerability of the buildings composing the HUBE is assessed through established methodologies, while the exposure assessment introduces more original elements.

Specifically, the assessment of the physical vulnerability is based on a building-scale application of the Flood Vulnerability Index (FVI) [-], whose validated methodology was originally proposed by Miranda and Ferreira, (2019) and refined by Davis et al. (2023). The FVI approach is selected as it provides a flexible and accessible tool for assessing vulnerability in historic urban areas, even where hazard or loss data are incomplete or unavailable. This makes it particularly suitable for the Italian context, where the resources available to public administration offices allow for the collection of detailed structural information at the

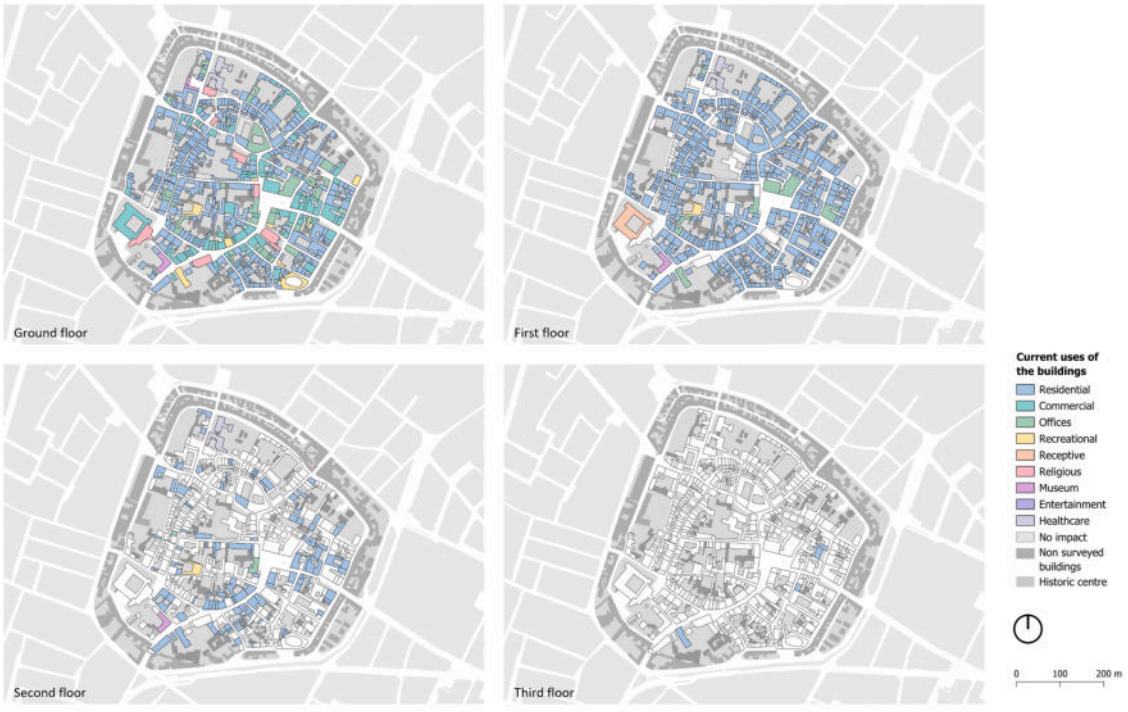

Fig. 4. Floor-level mapping of intended use across the surveyed buildings.

building scale, while hazard data are often unavailable, restricted, or difficult for local officers to interpret. According to this approach, the physical vulnerability of a building to a flooding event is assessed through the analysis of two primary components: the building Sensitivity Index (SI) [-], which quantifies the building's physical susceptibility to flood damage; and the building Exposure Index (EI) [-], which reflects the building's contextual and functional characteristics, including heritage value, but does not directly consider the number and typology of specific users hosted herein.

A total of ten parameters is used, of which seven are related to sensitivity and three to exposure, as shown in Table 1. Each parameter is classified into four vulnerability classes (A to D), associated with increasing levels of susceptibility and exposure. The corresponding weights - $A = 10$ (lowest vulnerability), $B = 40$, $C = 70$, $D = 100$ (highest vulnerability) – reflect the assumption that all historical buildings possess an inherent minimum vulnerability, even under the most favourable conditions. As a result, the weight of class A is not equal to 0, to denote that a minimum level of vulnerability is associated with traditional construction materials, ageing structures, and architectural configurations typical of HUBEs. The sensitivity parameters describe the structural, material and geometric characteristics that determine a building's susceptibility to floodwater intrusion. These elements include conservation state, structural and finishing materials, characteristics and number of openings, presence of basements, and threshold height—elements consistently recognised in previous FVI applications as key physical pathways for water intrusion and damage (Davis et al., 2023; Miranda & Ferreira, 2019). The exposure parameters account for potential economic, physical and cultural losses. The relative contribution of these three parameters within the EI follows the hierarchical weighting established in the FVI framework, reflecting their documented influence on economic disruption, local physical impacts, and cultural heritage loss.

Table 1
Flood Vulnerability Index: components, parameters, attributes, classes and weights (Davis et al., 2023).

Components	Parameters	Attributes	Class CV_i	Weight p_i
Sensitivity	S1	No damage/cracking	A	10
	State of conservation	Slight cracking (<0.5 mm)/moisture	B	40
		Generalised cracking (2–3 mm)/ settlements/erosion	C	70
		Deformation/serious material decay	D	100
	S2	Reinforced concrete/ steel structures	A	10
	Structural material	Masonry structures	B	40
		Timber structures	C	70
		Earth structures	D	100
	S3	Steel/concrete/glazed tile/glass	A	10
	Facades' finishing material	Brick/plaster/regular dressed stone	B	40
		Unglazed tile/ irregular stone/wood panels	C	70
		Earth/rubble stone	D	100
	S4	Plastics	A	10
	Window/door frames' type and condition	Metals	B	40
		Wood	C	70
		Total exposure	D	100
	S5	Without openings	A	10
	Openings on the ground floor	Window openings, without door openings	B	40
		Window and door openings	C	70
		Large openings	D	100
	S6	No basement	A	10
	Existence of basements	Basement without windows; no direct access	B	40
		Basement with windows; no direct access	C	70
		Basement with direct access	D	100
	S7	$\geq$ 2 steps	A	10
	Height of the door threshold	$<$ 2 steps	B	40
		Level with the outside	C	70
		−1 or more steps	D	100
Exposure	E1	Educational/dwelling	A	10
	Type of use/ activity	Commercial	B	40
		Restaurant	C	70
		Hotel/religious	D	100
	E2	Convex	A	10
	Surface condition	Flat and permeable	B	40
		Flat and impermeable	C	70
		Concave	D	100
	E3	Non-classified	A	10
	Buildings' heritage value	Non-classified of high public interest	B	40
		Local or national interest	C	70
		International interest	D	100

The FVI value is calculated as the product of the sensitivity and exposure components, according to Eq. (1):

$$FVI = (SI \times EI)/FVImax \quad (1)$$

Where FVI max is the maximum FVI value in the HUBE, considering the weights in Table 1.

In addition to FVI, two components are included to describe the exposure of buildings to potential flooding, depending on the conditions of the surrounding urban layout, respectively related to the water impact direction and the road width. These components are drawn on methodologies such as space syntax analysis (Hillier et al., 1976), which explores the relationship between urban morphology and risk, and has been applied to approaches from seismic research (Cremonini, 2004; Giuliani et al., 2020), which are herein adapted to study flood vulnerability in HUBEs. To evaluate these components, the street network is simplified into a parametric graph composed of nodes (defined at intersections, profile changes, or width variations) and links (road network elements between nodes). Each building is connected to the faced link, so that the geometric attributes of the road (e.g. width, flow direction) can be assigned to the building within the GIS database. This framework allows for a systematic assessment, where water direction and street width become exposure indicators, respectively defined by the Flood Direction Exposure (FDE) [-] and Road Width (RW) [-] indexes.

The FDE index quantifies the potential impact of water flow on each building. For each street in the HUBE, two opposite flood directions are considered: C1, representing water flowing in one direction (e.g., right → left), and C2, representing water flowing in the opposite direction (e.g., left → right).

For both C1 and C2, each building is classified into three levels of exposure based on its orientation:

1. low exposure →parallel impact: water flows alongside the building;
2. moderate exposure →angled impact: water flows obliquely against the building;
3. high exposure →perpendicular impact: water flows directly into the building.

The exposure levels from C1 and C2 are combined using a 3 × 3 matrix, producing a final exposure classification (FDE) for each building on a 1–5 scale, as reported in Table 2. Finally, to normalise the FDE index, each building's value is divided by the maximum possible value (5), resulting in a dimensionless indicator [-].

Finally, the RW indicator reflects the influence of road width on flood severity parameters such as water velocity, pressure and depth,

Table 2
Flood Direction Exposure (FDE): classification of exposure levels based on a 3 × 3 matrix depending on two possible flood direction scenarios C1 and C2.

FDE		C1		
		low	moderate	high
C2	low	1	2	3
	moderate	2	3	4
	high	3	4	5

given the conditions of the case study (Balaian et al., 2024; Mignot et al., 2019). As noted in Section 4.1, none of these hazard-related parameters is directly considered in this study. Instead, RW serves as a proxy for the potential exposure of each building based on the geometry of its surrounding urban layout. This approach aims to identify the roads – and the buildings along them – that are more susceptible to such effects compared to others. Hence, for each road, RW is calculated as the ratio between the road width and the maximum road width in the HUBE, thus ranging from 0 (excluded) to 1 (for the maximum road width in the HUBE).

It is important to note that FVI, FDE and RW are "static" for the purpose of the present analysis. Their values are derived from intrinsic features of the built environment, such as construction typology, material degradation, and location-specific exposure conditions, which do not exhibit significant variations at the temporal scale relevant to this study (i.e., daily and sub-daily timespans). On the contrary, the user exposure and vulnerability (addressed in Section 4.3) are defined as "dynamic" due to their dependence on the number, distribution and characteristics of individuals over time. Consequently, building-related variables are treated as time-invariant inputs within the assessment framework, providing a stable baseline against which the effects of temporal variability in user-related components can be meaningfully and innovatively evaluated.

4.3. Dynamic modelling of user exposure and vulnerability

The exposure and vulnerability of users, along with their temporal variations, are assessed using methodologies established in previous research (Bernardini et al., 2024; Quagliarini et al., 2023), by innovatively adapting outcomes to the microscale. The analysis focuses on quantifying and characterising users within the case study area through a structured approach that considers both the geometric and functional attributes of buildings, to ensure rapid application by decision makers and technicians.

The first step involves assessing the intended use of the building. The input data was derived from GIS sources, which provide information on the intended use and geometric characteristics of buildings, including covered area and the number of floors. Intended uses are first organised into five use classes (Salvalai et al., 2022), considering both the function of the building and the main individual characteristics of its occupants. Each use class is further characterised by its potential vulnerability, through the use-vulnerability weight w_{use} [-] defined considering the typology of users who could be hosted herein, in terms of possible sensory/motion impairments, general age features, and familiarity with the built environment. Such weights are innovatively defined by the current work to reflect user vulnerability not only based on physical condition, but also psychological and knowledge-based factors influencing evacuation behaviour and risk perception. In particular, this study adopts a proportional weighting scale ranging from 0.2 to 1, applied at regular intervals, thereby ensuring an effective differentiation of priority levels among use classes. This systematic and evenly spaced weighting scale reflects the functional and strategic role each use class plays in the overall vulnerability assessment. More sensitive and critical use classes have a stronger influence on the final assessment, while less vulnerable categories have a proportionally reduced impact (Papathoma-Köhle et al., 2019). By employing regular interval weighting scales, this approach enables a rigorous and easily interpretable assessment of vulnerability, offering a flexible framework that captures the complexity of heterogeneous urban environments while remaining adaptable to diverse social and spatial conditions (Agliata et al., 2022; Moreira et al., 2021; Papathoma-Köhle et al., 2019). As presented in Table 3, w_{use}=1 is assigned to the "Sensitive" use class, composed of healthcare facilities and schools, due to the presence of children, elderly people, or patients, who typically exhibit higher vulnerability and lower familiarity with emergency procedures (Abigail et al., 2018; Ellena et al., 2020). Other relevant w_{use} values are assigned to "Services and Culture" use class, considering the possible presence of many users who are not familiar with the building and the HUBE, such as visitors and tourists (Mao et al., 2019). Lower w_{use} values are associated with use classes mainly hosting workers and residents (Macintyre et al., 2018), who potentially have a higher level of knowledge and awareness of the HUBE, the safety procedures and the flood risk conditions.

To estimate occupancy, each intended use is associated with a standard occupant load factor [pp/m^2] representing the typical density of users per unit area, essentially derived from fire safety codes, cross-checked against previous applications in comparable urban contexts to ensure consistency (Bernardini et al., 2024). These values are applied to the gross surface area of each intended use of each building to estimate the number of occupants. Table 3 summarises the five use classes considered in this sudy, together with the associated occupant load factors and time-based occupancy profiles. These temporal variations are a critical component of the method, enabling user exposure to be modelled as a "dynamic" variable that changes throughout the day according to the building's function, typical use patterns, and accessibility (Quagliarini et al., 2023; Salvalai et al., 2022). In Table 3, garage areas for public and private uses are not considered, assuming that there is no occupant load over time, and that occupants eventually placed herein are those that populate the related main areas of the buildings. This assumption is also coherent with recommendations by Civil Protection Bodies on safety behaviours in garage areas placed in underground spaces (Guidelines for flood risk), which are recognised as critical flood entry points and potential sources of risk, where evacuation procedures could be slowed down or hindered. Nevertheless, when underground infrastructures host regular users (e.g. accessible parking or station areas), occupancy assumptions can be refined accordingly to improve the accuracy of exposure estimates (He et al., 2024; Wu et al., 2025).

The approach described above could provide conservative results on the number of occupants since the occupant load factors are: (1) standardised and devoted towards maximum crowding indexes, thus not allowing to represent specific operational contexts with more limited exposure (especially in view of seasonal occupancy variations, e.g. in holiday periods for residential and business buildings); (2) are applied to the gross area. Nevertheless, it provides an efficient approach for exposure assessment and allows for the derivation of context-specific load factors using the same methodological rationale, depending on the specific building conditions. This parametrisation aims to balance efficiency and methodological conservation by adopting maximum-occupancy scenarios to consider potential worst-case conditions, ensuring to focus on prioritisation of mitigation strategies in critical situations. Otherwise, the occupant load factor could also be refined based on specific areas of the building or applied to net usable areas (e.g. living environments or working spaces), thus reducing potential overestimation associated with the use of gross floor area. In addition, corrective factors to occupancy load and daily timetable could also be introduced in view of seasonal variations of use, especially in the case of available in-situ surveys and detailed data. These corrective factors could indeed amplify occupant loads, considering that the user flows may further amplify exposure dynamics, particularly in heritage cities with high touristic relevance, in case of temporary events and mass-gatherings (Quagliarini et al., 2023).

Users are then classified by age group, as age significantly influences

Table 3
Classification of buildings by use class (as defined in Salvalai et al. (2022)), intended use, corresponding occupant load (in view of the application contexts, the Italian Fire Prevention Code, D.M. 3 August 2015, is assumed, being consistent with previous works (Quagliarini et al., 2023)), daily timetable and use-vulnerability weight.

Use classes (definition and references)	Intended use	Occupant Load [pp/m^2]	Daily timetable	Use-vulnerability weight: *wuse* [-]
Sensitive: Facilities intended for social assistance or healthcare functions, where the concentration of individuals with age- or health-related fragilities increases local vulnerability (Abigail et al., 2018; Ellena et al., 2020).	Healthcare (hospitals, nursing homes, social welfare facilities)	0.4	0–24	1.0
	Schools	0.4	8–13	
Services and Culture: Buildings and spaces attract users through cultural, leisure, or social interaction opportunities; often air-conditioned, they can serve as strategic shelters for sensitive users (Mao et al., 2019).	Commercial (shops)	0.4	8–19	0.8
	Recreational (bars and restaurants)	0,7	8–21	
	Entertainment (cinemas, theatres)	1.2	8–21	
	Museums	0.7	8–19	
	Religious	0.7	8–19	
	Universities	0.4	8–19	
	Sport (gyms, sports centres)	0.4	8–19	
Business: Buildings open to the public and used for administrative, professional, or commercial service activities, generally characterised by moderate user density and predominantly worker presence (Mao et al., 2019).	Offices (banks, insurance, research centres, private offices, professional studies etc.)	0.4	8–19	0.6
Production: Buildings mainly dedicated to private or restricted-access productive activities, with controlled entry limited to authorized personnel.	Factories, labs etc.	0.1	8–19	0.4
Residential: Housing units whose exposure depends on their spatial placement and construction features; typically occupied by permanent residents (Macintyre et al., 2018).	Receptive structures (hotels etc.)	0.4	0–24	0.2
	Residential (homes, colleges, monasteries etc.)	0.05	0–24	

both spatial and temporal behaviour patterns. The population is grouped into demographic categories: toddlers (0–4 years), parent-assisted children (5–14 years), young adults (15–19 years), adults (20–69 years), and the elderly (70+ years) (Quagliarini et al., 2023). The demographic characterisation of the population can be obtained from local registers or census databases. These datasets, freely available and updated annually, provide detailed information on age distribution, offering a comprehensive overview of the population structure within the study area.

The age-related classifications provide insights into how different age groups use space over time, enhancing the temporal resolution of user exposure estimates (Quagliarini et al., 2023; Renner et al., 2018). It is assumed that toddlers and the elderly remain at home throughout the day, while school-aged children and young users are generally away between 08:00 and 13:00. Adults are not considered at home from 08:00 to 18:00 due to work or university activities. These assumptions are based on typical local daily activity patterns and opening hours of offices, shops, and public services in central Italy, as well as standard working hours (Bernardini et al., 2024; H. Chen et al., 2022; Renner et al., 2018). Incorporating these local temporal dynamics into the exposure assessment enables a more realistic and context-specific estimation of population presence and vulnerability (Bernardini et al., 2024; Quagliarini et al., 2023).

On these bases, the exposure E [-] is first calculated as the ratio between the number of users associated with the intended uses of the entire building, and the number of users corresponding to the maximum occupancy density (e.g. the maximum one in Table 3, or those corresponding to the maximum occupant load in the assessed HUBE). When the density reaches the set limit, E is capped at 1.0 to prevent overestimation issues.

According to previous works, for each building, three indicators have been identified to characterise the overall users' vulnerability UV [-]:

UV_a - Age-related vulnerable users [-]: assesses the proportion of users considered more susceptible to risks due to age-related factors, particularly toddlers, parent-assisted children, and elderly users. It is calculated as the ratio between the number of users classified as age-vulnerable (U_{age}) [pp] and the total number of exposed users within the building (U_{tot}) [pp], as expressed in Eq. (2):

$$UV_a = \frac{U_{age}}{U_{tot}} \tag{2}$$

UV_p - Flood-vulnerable users [-]: quantifies the proportion of exposed users located on the ground floor relative to the total number of users within the building. It is computed as the ratio between the total number of users present on the ground floor of the buildings in the study area (U_{gf}) [pp] and the total number of exposed users within the building (U_{tot}) [pp], as shown in Eq. (3):

$$UV_p = \frac{U_{gf}}{U_{tot}} \tag{3}$$

In this way, the index assesses the direct flood effects on users, as

those located on the ground floor would need to evacuate or move to higher levels in case of a flood event.

UV_u – Vulnerable users by intended use [-]: assesses the proportion of exposed users based on the building's intended use. It is calculated as the weighted sum of the ratio between the number of users associated with a specific intended use (assigned to each floor of the building) and the total number of users within the building, as given by Eq. (4):

$$UV_f = \sum w_{use} \frac{O_{use}}{O_{use,tot}} \quad (4)$$

where O_{use} represents the number of users assigned to a specific intended use on each floor [pp], $O_{use,tot}$ is the total number of users in the building [pp], and w_{use} is the weight factor [-] shown in Table 3.

Each of the E and UV indicators is treated as a time-dependent parameter, reflecting changes in occupancy and user distribution across different hours of the day. This "dynamic" representation enhances the robustness of the analysis by enabling the identification of critical time intervals during which user exposure and vulnerability could reach their peak. Moreover, it ensures methodological consistency and facilitates comparability across different spatial configurations and evaluation scenarios (Bernardini et al., 2024; Salvalai et al., 2022).

Finally, all user-related exposure and vulnerability factors are considered continuous, ranging from 0 to 1. The minimum value (0) is reached only for uninhabited buildings in a permanent way (e.g. abandoned buildings) or in given times of the day (e.g. during closure times of public buildings), being consistent with the assumption that no effects of E and UV could exist in case no user is present.

4.4. Aggregation and comparison of vulnerability and exposure indicators

Physical Vulnerability (PV) [-] and User Vulnerability and Exposure (UEV) [-] indexes are then calculated by aggregating the specific indicators defined respectively in Section 4.2 and Section 4.3, using a Weighted Linear Combination Method (Agliata et al., 2022), where each basic parameter is associate to a weight, calculated through the application of the Analytical Hierarchy Process (AHP) (Dong et al., 2010; Goepel, 2018). AHP is a multi-criteria decision-making approach recognised in flood risk assessment that allows a consistent and transparent integration of heterogeneous parameters (Agliata et al., 2022; Ashfaq et al., 2025; Huang & Feng, 2025; Malekinezhad et al., 2021; Papathoma-Köhle, 2016). Two distinct AHP analyses were performed, one for PV and one for UEV, to reflect the conceptual separation between structural fragility and user-related dynamics and the possibility to additionally integrate them in an integrated index. The PV index is obtained by the weighted aggregation of the FVI, FDE, and RW parameters (Section 4.2), while the UEV index is obtained by aggregating the parameters E, UVa, UVp, and UVu (from Section 4.3), as summarised in Fig. 5.

In particular, the AHP Excel system (Goepel, 2018) is used to derive the weight values for each factor within the PV and UEV indexes, based on the pair-wise comparison on a linear integer scale ranging from 1 (same importance) to 9 (maximum importance of the considered risk factor with respect to the others). The final priorities, calculated through the row geometric mean method (RGMM) (Goepel, 2013), have then been normalised so that their sum equals 1 for each assessed single risk. According to reference works (Bernardini et al., 2024), the pairwise comparison has been performed by a group of experts. In particular, seven volunteers selected among research group universities and having different backgrounds in flood risk, urban planning, and social vulnerability were involved in this step. According to the AHP approach (Dong et al., 2010; Goepel, 2013), the Consistency Ratio (CR) represents the standard measure for verifying the logical coherence of the pairwise comparisons, with a threshold of 10 % generally accepted as the validity criterion.

Hence, individual pairwise comparisons among PV and UEV factors, and thus the outcoming matrices, are then aggregated to form a group consensus matrix using the RGMM prioritisation method (Dong et al., 2010; Goepel, 2013). This process ensures that the final weights reflect a balanced synthesis of multiple expert perspectives, while the consistency ratio is calculated for each matrix to verify the logical coherence of the judgments. In particular, all individual and aggregated AHP demonstrated a CR<10 %, confirming the validity of the pairwise comparisons. CR=2.1 %<10 % for PV index and CR=0.4 %<10 % for UEV index. Then, the level of agreement among decision-makers has been assessed through the AHP consensus indicator S*, a homogeneity index based on Shannon entropy (Goepel, 2013, 2018). S* values range from 0 % (no consensus) to 100 % (full agreement), with higher values indicating stronger alignment among evaluators. The S*=98 % for PV and S*=75 % for UEV confirm a strong level of agreement among decision-makers, despite their different expertise and backgrounds, supporting the robustness and credibility of the resulting weighting scheme. For any additional details on the calculation of consensus group indexes, please refer to the reference work (Bernardini et al., 2024) (i.e. see Appendix A).

The final formulation of the PV and UEV indices is obtained through a weighted linear combination of the parameters, using the weights established through the AHP method, as shown by Eqs. (5–6).

$$PV = 0.66 * FVI + 0.235 * FDE + 0.105 * RW \quad (5)$$

$$UEV = 0.075 * E + 0.434 * UV_a + 0.309 * UV_p + 0.182 * UV_u \quad (6)$$

This dual-structure formulation allows for an explicit distinction between the intrinsic physical vulnerability of buildings and the "dynamic" vulnerability of the hosted users. Maintaining this separation before integration enables a clearer interpretation of the relative influence of physical and user components, while supporting targeted mitigation and preparedness strategies. According to Section 4.2 and Section 4.3, components of these indices are normalised, varying from 0 to 1, and thus the final PV and UEV indices would also vary within the same range (according to Eq. (3) and Eq. (4) definitions), allowing the aggregation of heterogeneous indicators and enabling consistent interpretation over space and time. To facilitate interpretation, PV and UEV indices are classified into five levels: 0.0≤negligible<0.2; 0.2≤low<0.4; 0.4≤moderate<0.6; 0.6≤high<0.8; 0.8≤extreme≤1.0. This discretisation is widely adopted in flood risk assessment since it converts continuous vulnerability values into categorical classes, enhancing clarity, comparability and accessibility for decision-makers (Evans et al., 2024; Taramelli et al., 2022).

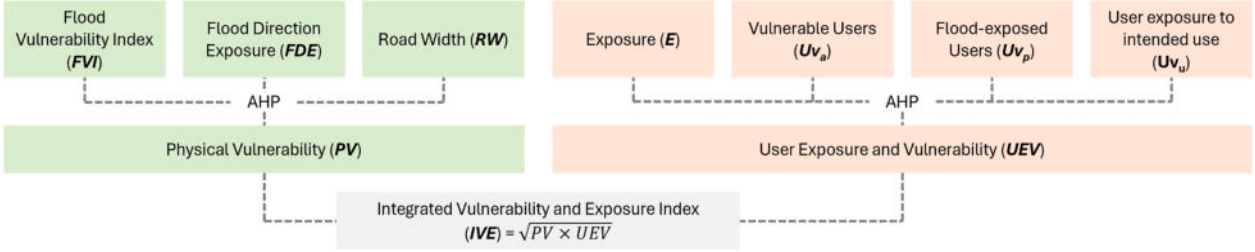

Fig. 5. Scheme of the composition of the PV and UEV indices and the final risk indicator.

The Integrated Vulnerability and Exposure Index (IVE) [-] is then calculated through the aggregation of the two normalised indices, PV and UEV, using the square root of their vector product, as illustrated in Eq. (7):

$$IVE = \sqrt{PV \times UEV} \tag{7}$$

This formulation has been selected for different reasons. While the traditional multiplication-based approach remains theoretically valid, this adjusted formulation provides enhanced sensitivity and interpretive robustness, particularly in heterogeneous urban contexts (Daníelsson & Zigrand, 2006; Hamasha et al., 2022). In this sense, considering the current case study application, the traditional direct product (PV x UEV) resulted in very wide variability: a few very large, high-density buildings (e.g., the hospital and the ex-convent with restaurants) showed values which were sensibly higher than the others, exacerbating vulnerability and exposure conditions. The square root transformation moderates these effects, yielding a more balanced and realistic distribution of vulnerability and exposure across the built environment. It also reduces the compensatory effects between PV and UEV, ensuring that buildings characterised by concurrent moderate values in both components are adequately represented. Furthermore, no weighting factors were introduced in the integration process, to preserve the proportional influence of PV and UEV within the combined index. This choice hence allows to combine "static" (building-related) and "dynamic" (user-related) components, supporting the interplay of social, ecological, and technological factors generating complex and context-specific vulnerability patterns (Sharifi, 2023).

PV, UEV and IVE values are then presented in GIS-based maps that illustrate the spatial distribution of each individual and integrated components, using the same five uniform levels proposed for PV and UEV, to make them consistent according to homogeneous classification rules defined above.

Finally, to evaluate the relative influence of the PV and UEV components on the overall integrated assessment, a comparison has been conducted between the aggregated risk values calculated with and without the inclusion of the UEV component. Comparison between IVE and PV comprises the definition of risk maps of the HUBE. This is achieved by calculating the percentage differences dIVE [%] in the overall risk index according to Eq. (8):

$$dIVE = \frac{IVE - PV}{PV}[\%] \tag{8}$$

dIVE hence mainly quantifies the influence of user-related dynamics (UEV) on the integrated index (IVE). Positive values of dIVE indicate that UEV significantly impacts risk, highlighting buildings where dynamic occupancy patterns and user vulnerability play a crucial role. Instead, negative dIVE values suggest that structural characteristics (PV) are the primary driver, with a reduced effect of user presence. This continuous indicator enables a more comprehensive understanding of interactions between physical and user vulnerability components within the urban fabric.

The use of a GIS environment supports the integration of spatial and descriptive data, allowing for spatially explicit analysis and

The use of GIS-based maps further enhances this interpretative capacity by spatially representing both individual components and their combined effect on the overall assessment, being ready for visualisation of multi-scale risk patterns, too. As also remarked by previous research (Bernardini et al., 2024; da Silva et al., 2022), this spatially explicit framework and GIS-based approach are able to support the identification of critical "hot spots" and priority areas for intervention. This strengthens the replicability to other urban contexts, by enhancing its relevance for decision-makers engaged in risk governance and urban planning, thanks to a direct connection between analytical results and practical insights.

5. Results

This section summarises the results from the leading indicators on PV and UEV, by providing insights into specific components that affect the outcomes. Extended content to support the results is also provided in Appendix A.

PV results, obtained through the aggregation of FVI, FDE and RW results, are mapped in Fig. 6. To maintain the compactness of the paper, the extended results of each PV component are presented in Appendix A. Specifically, the Flood Vulnerability Index (FVI) is shown in Fig. A1, the Flood Direction Exposure (FDE) in Fig. A2, and the Road Width (RW) in Fig. A3.

As shown in Fig. 6, most of the buildings fall within a physical vulnerability and exposure level ranging from low (0.2–0.4) to moderate (0.4–0.6). In general, this suggests that the expected physical impact of a flooding event on the structural integrity of these buildings is likely to be low to moderate. Despite this overall trend, it is essential to note that, although damage or losses cannot be directly estimated from these results, they enable the identification of specific buildings that may be more susceptible to damage. Namely, those buildings can be associated with higher PV values, and thus they should be prioritised for more detailed analysis and, if necessary, retrofit interventions.

The spatial analysis of the results has also revealed that buildings classified as having higher PV values are predominantly located along the HUBE major streets, highlighting a clear link between vulnerability classes and urban organisation features. Palaces along the main road, with large openings, tend to be more vulnerable, while buildings on narrower streets—typically smaller, simpler terraced or row houses with narrow fronts—show lower vulnerability levels. Moreover, buildings on the oldest streets, as well as those on the main squares, are classified as more vulnerable due to their heritage designation. Many buildings have steps in front of the main entrance, which can help prevent water from entering. As those can be found in a significant percentage of buildings, they could be interpreted as a vernacular mitigation measure, reflecting an adaptive architectural response to floods. The widespread curvature of the street network contributes to average FDE values (Fig. A2 in Appendix A). However, buildings positioned perpendicularly to the street direction are more exposed, as they directly face the flow of incoming water. Their vulnerability is, however, partly offset by the RW parameter, which considers wider open areas, such as squares, as less vulnerable. Taken together, the results indicate that the distribution of building vulnerability is closely related to the configuration of the road network, with consistent patterns emerging across both sets of analyses. This outcome is partly due to the harmonisation process, which prioritised the intrinsic vulnerability of buildings represented by FVI, while assigning relatively lower weights to flood direction exposure FDE and road width RW, as reported in Eq. (5).

As outlined in Section 4.3, unlike the PV, which is represented by a "static" component and is therefore illustrated through a single map visualisation, user exposure and vulnerability are considered "dynamic" and hence variable throughout the day. They are therefore analysed across the defined time intervals. The following figures show the maps related to the indicators E, UVa, UVp, and UVu, respectively, in Fig. 7, Fig. 8, Fig. 9, Fig. 10. The results are presented in 4 different panels organised according to the time intervals defined in Section 4.1.

Fig. 7 represents the spatial distribution of E values, which are generally low across the study area. This pattern reflects the overall homogeneity of user exposure, primarily associated with the predominance of residential land uses. Peaks of high to extreme values are observed in buildings hosting recreational activities (e.g., bars and restaurants), entertainment (e.g., cinemas and theatres), museums, or religious purposes, particularly during morning and afternoon, which correspond to the typical opening hours of these public activities. As outlined in Section 3, the prevalence of residential buildings, which comprise 67 % of the study area and are primarily characterised by low-rise housing, contributes to this phenomenon. The effect is particularly

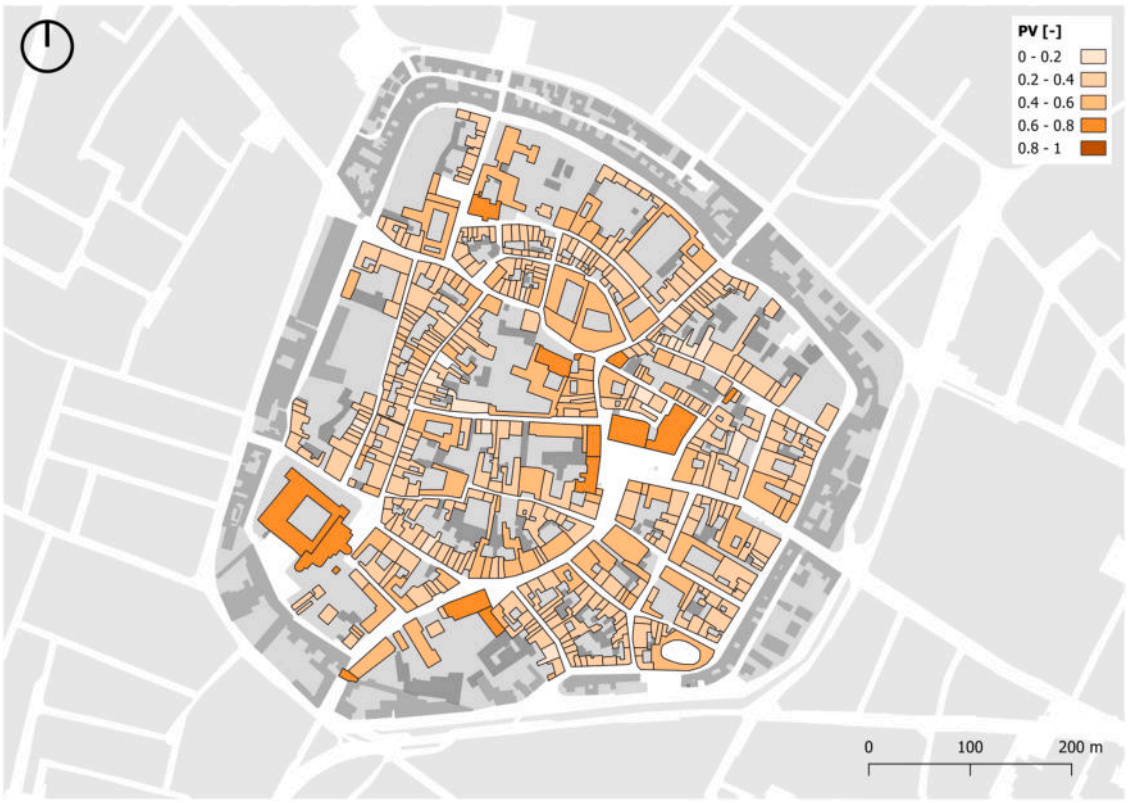

Fig. 6. Map of PV values, according to the general classification ranges adopted for all the indicators in this work.

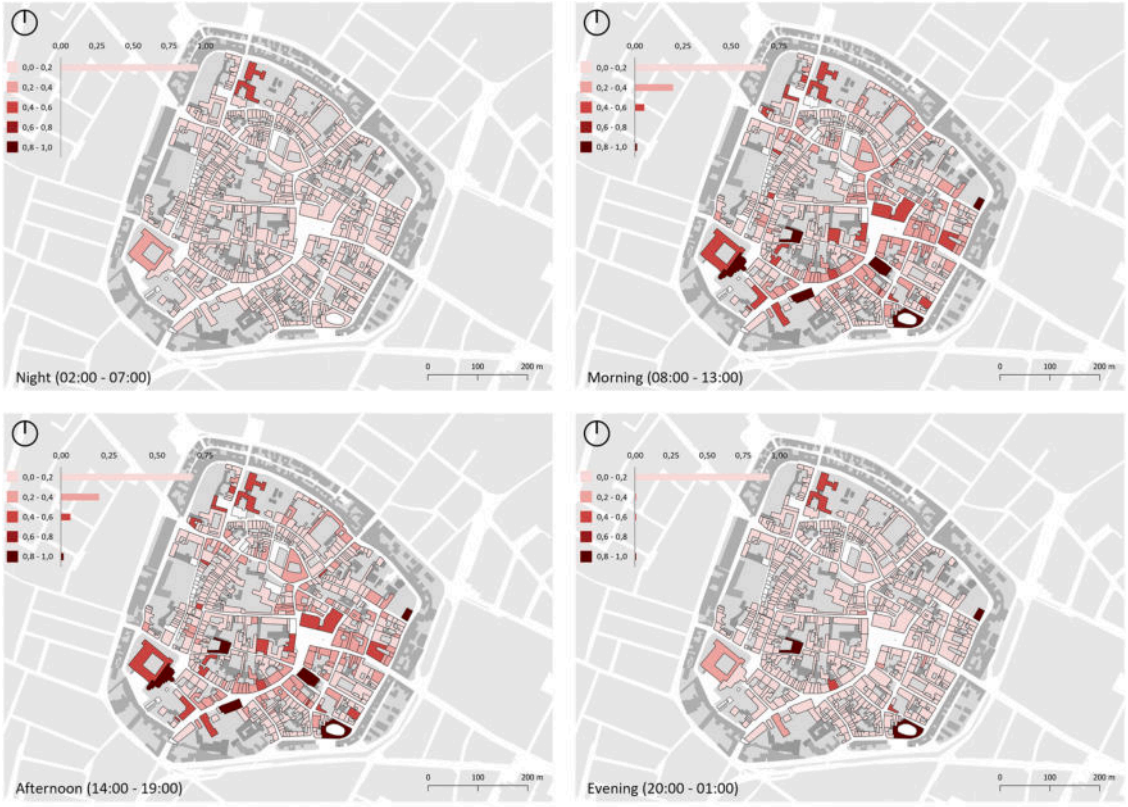

Fig. 7. Maps of E over time, classified according to the general ranges adopted in this study, with bar charts showing the proportion of buildings in each class for the different time slots.

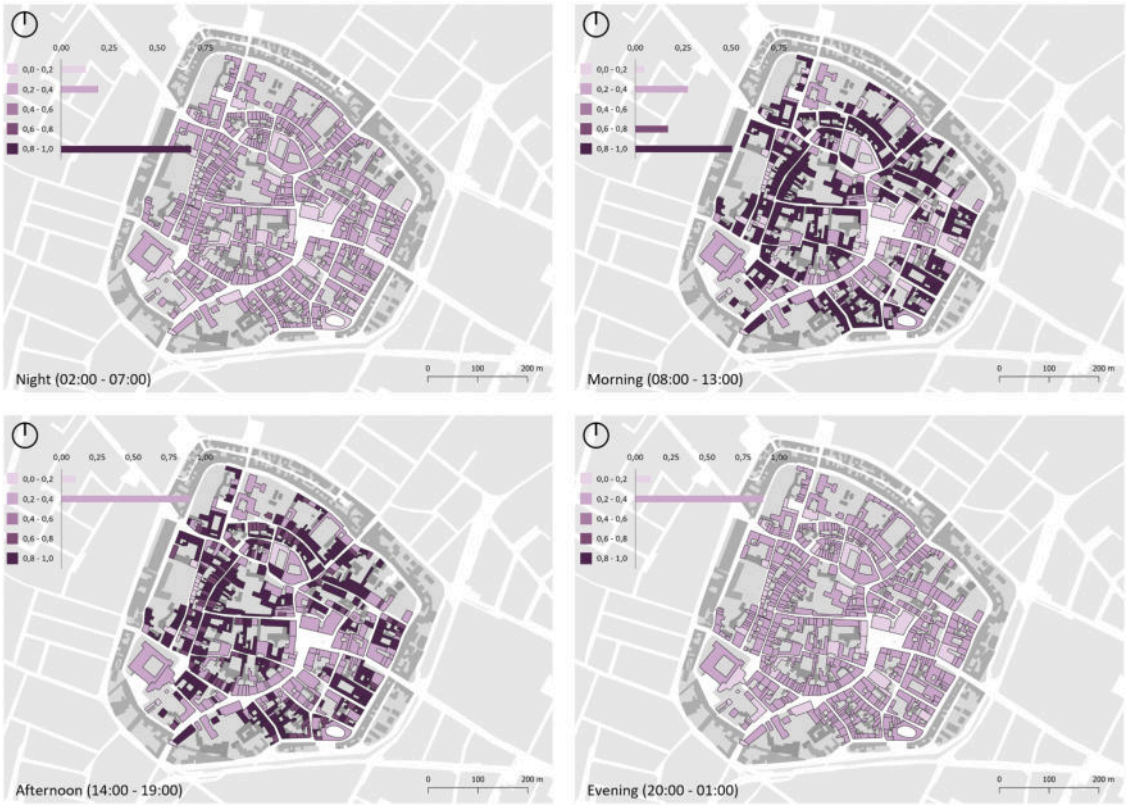

Fig. 8. Maps of UVa over time, classified according to the general ranges adopted in this study, with bar charts showing the proportion of buildings in each class for the different time slots.

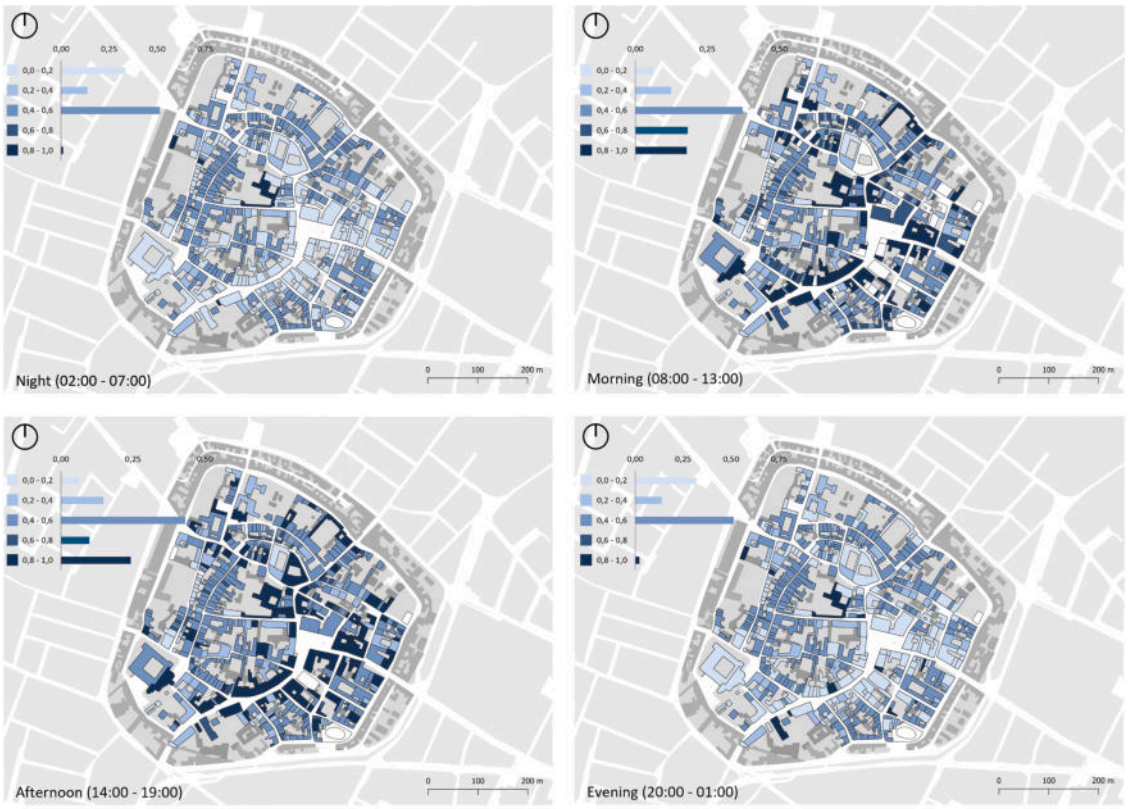

Fig. 9. Maps of UVp over time, classified according to the general ranges adopted in this study, with bar charts showing the proportion of buildings in each class for the different time slots.

Fig. 10. Maps of UVu over time, classified according to the general ranges adopted in this study, with bar charts showing the proportion of buildings in each class for the different time slots.

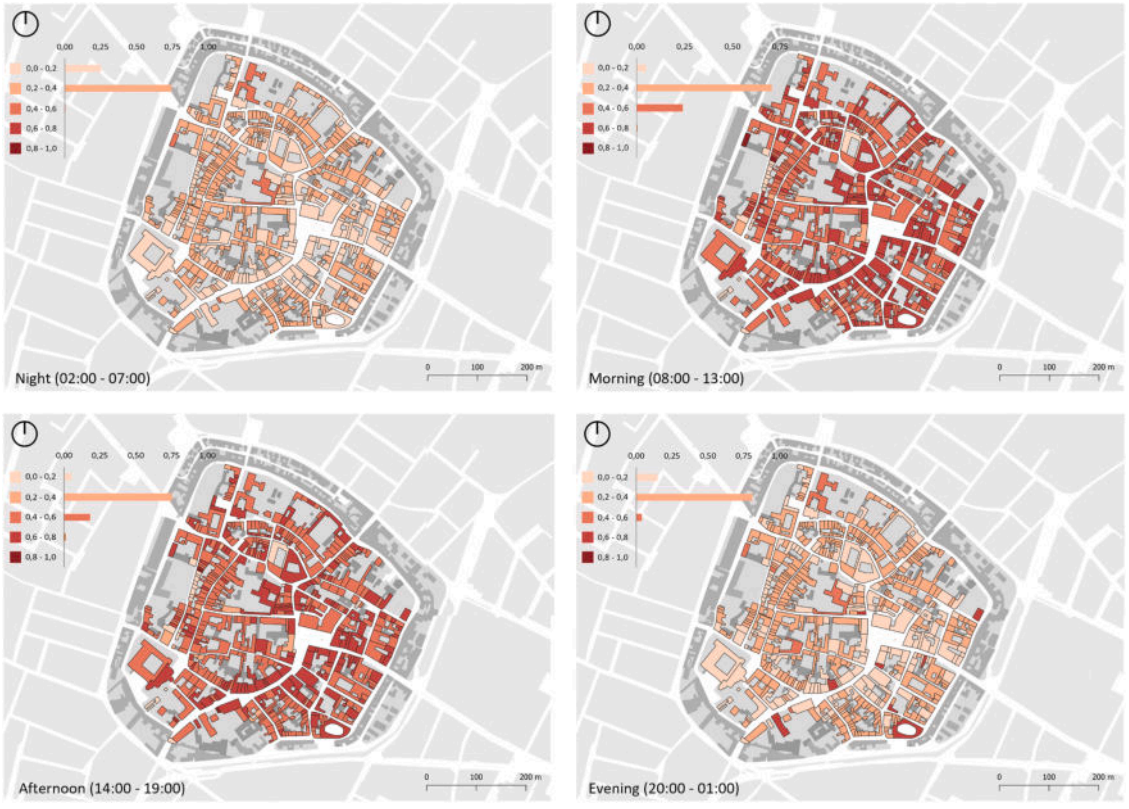

Fig. 11. Maps of UEV over time, classified according to the general ranges adopted in this study, with bar charts showing the proportion of buildings in each class for the different time slots.

pronounced during evening and night-time intervals, when it is assumed that all users are at home and the majority of non-residential activities are closed.

Similarly, temporal variations of UVa (Fig. 8) are influenced by the dominance of residential use. An apparent variation in UVa values can be observed between day and night, as expected, given the assumptions about occupancy schedules defined in Section 4.3. In particular, during the morning and afternoon intervals, residential buildings are predominantly occupied by users belonging to vulnerable age groups (i.e., toddlers, parent-assisted children, and the elderly). This variation is further reinforced by the limited area occupied by other intended uses within the study area, which have a negligible influence on this parameter.

Otherwise, significant variations over time can be observed for the UVp maps (Fig. 9). As expected, the night and evening intervals have the lowest impact, since most activities occupying ground floors and open to the public (e.g., shops, bars, restaurants) are closed. In addition, several residential buildings have a garage on the ground floor, and these spaces do not contribute to user presence, as stated in Section 4.3 assumptions. The morning and afternoon intervals show the most critical conditions in UVp, with values that vary slightly yet remain comparable, reflecting the typical opening hours of the various activities in the area, indeed.

The UVu maps (Fig. 10) reveal a significant variation between night-time, when most users remain at home, and the other periods of the day, which show increased vulnerability due to higher user concentrations in non-residential uses, particularly those classified as sensitive. For instance, the hospital located in the northern part of the HUBE, identified as a "sensitive" (Table 3), shows extreme UVu values across all time intervals, indicating the potential presence of vulnerable users (including those with sensory and motion impairments). Similar trends are observed during the daytime, with peaks reaching high levels during the opening hours of functions classified under "Services and Culture" (e.g. restaurants in the evening) due to the presence of non-familiar users. Such conditions significantly contribute to vulnerability, especially in flood scenarios or other emergencies.

The aggregated UEV index (Fig. 11) reflects the trends observed in its components. The evening and night-time intervals display predominantly minimal to moderate values, with a relatively uniform distribution, particularly across residential buildings, where conditions remain consistent throughout the day. Higher values are primarily associated with buildings hosting non-residential functions, especially in the morning and afternoon intervals, which correspond with the opening hours and the presence of sensitive functions.

The IVE maps (Fig. 12), calculated by integrating PV and UEV parameters, demonstrate significant temporal variability. As expected, the night-time interval presents the lowest IVE levels, with only a few isolated buildings reaching moderate values. Conversely, during the other time intervals, several more buildings with moderate IVE levels can be observed, with high-risk peaks occurring in the morning and afternoon. This finding underscores the importance of exposure and user vulnerability (UEV) during daytime periods in the context of flood risk assessment. However, in the case study, PV and UEV values for individual buildings often diverge, resulting in a compensatory effect between the two parameters in the final calculation. In other words, according to the comparison of Fig. 6 and Fig. 11, buildings with higher PV are often characterised by lower UEV, balancing the overall conditions of buildings in terms of vulnerability and exposure, and vice versa.

The specific impact of UEV on the risk and the presence of temporal dynamics are clearly illustrated by the maps of dIVE values shown in Fig. 13. This figure compares overall risk with and without UEV, thus comparing IVE outcomes from Fig. 12 with PV outcomes from Fig. 6. When dIVE > 0, the colours in Fig. 13 move towards red, as long as the risk levels are more prominent when considering UEV in conjunction with PV. Conversely, when dIVE < 0, colours move towards green, demonstrating that the integrated assessment based only on PV is more conservative and including UEV leads to a decrease in the expected IEV

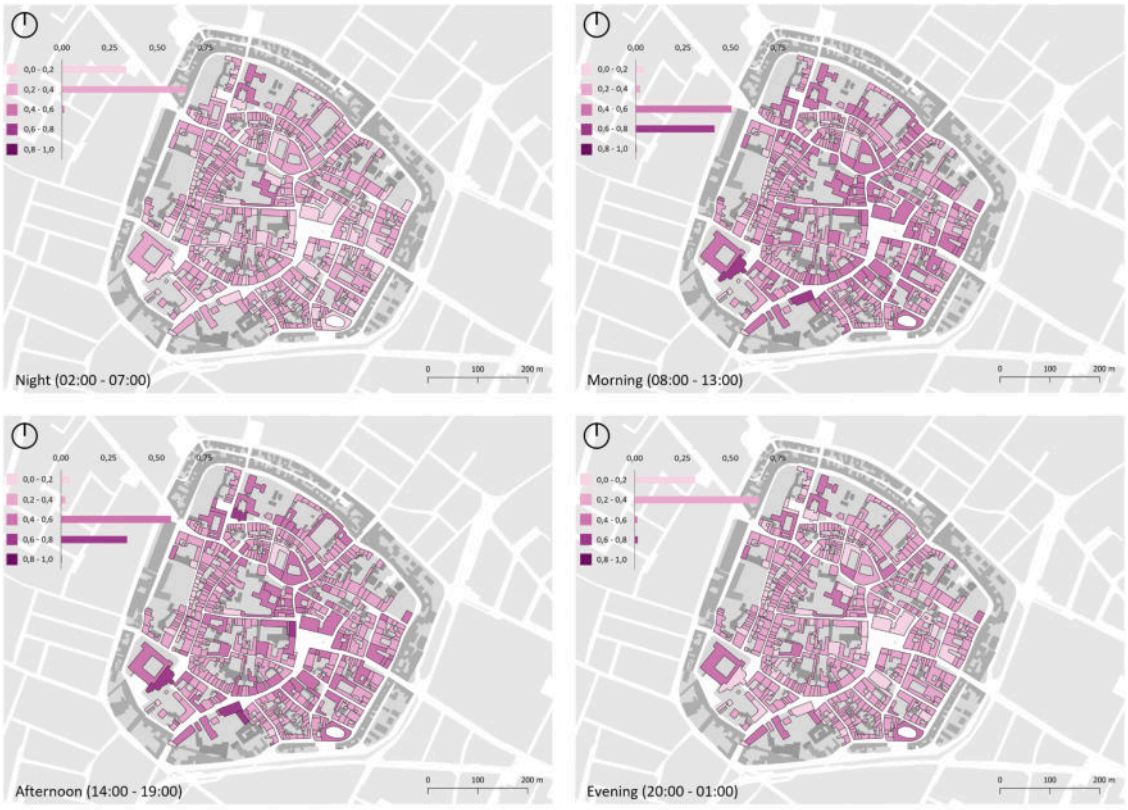

Fig. 12. Map of IVE over time, classified according to the general ranges adopted in this study, with bar charts showing the proportion of buildings in each class for the different time slots.

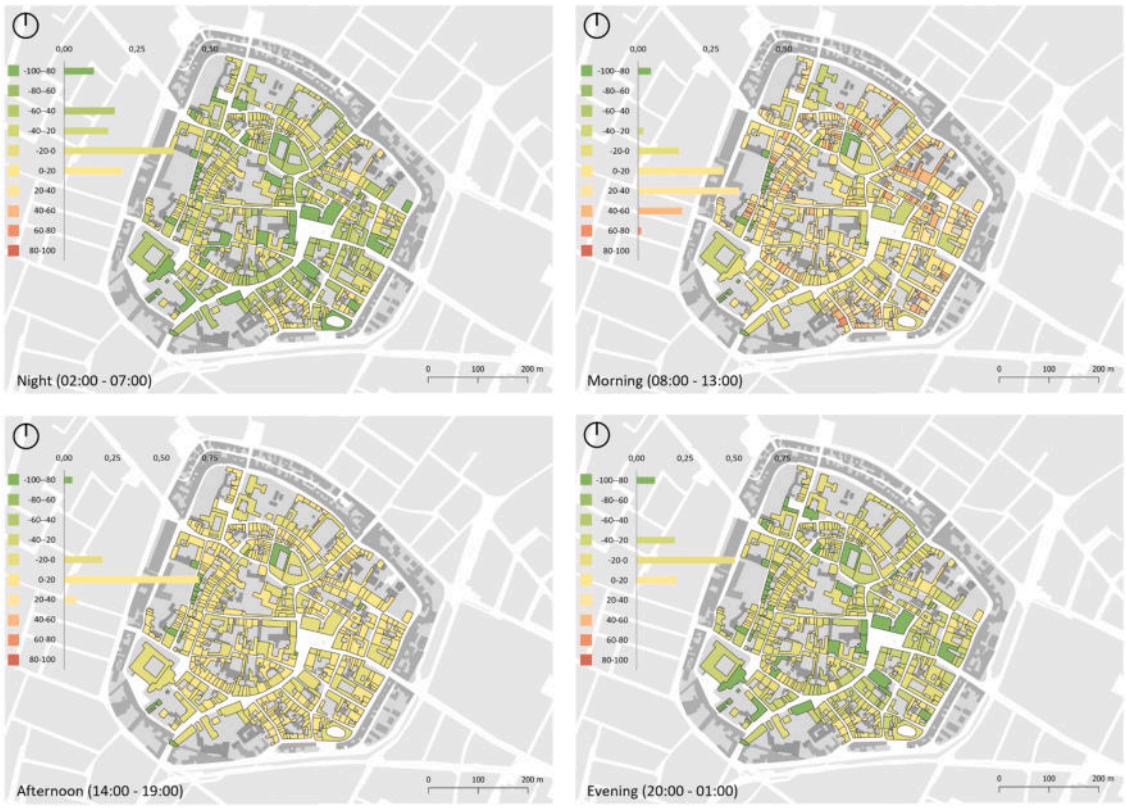

Fig. 13. Maps of dIVE over time, comparing the integrated Vulnerability and Exposure with (yellow to red gradient – referring to IVE as function of PV and UEV) and without (yellow to green gradient – only referring to PV) user-related components. Bar charts show the proportion of buildings in each class across the different time slots.

value. Given the above, in buildings hosting residential and, eventually, public functions at the lower levels (e.g. shops, restaurants, offices), UEV tends to dominate over PV, especially during the morning hours (highlighted in orange, thus implying an increase of risk due to UEV inclusion in the final risk levels. On the contrary, in relevant building heritage, especially in buildings associated with the "Services and Culture" class as the leading intended use, such as museums or churches, PV exerts a greater influence on the overall integrated assessment. As also shown by Appendix A, this outcome is mainly due to the highest significance, in the HUBE, of their FVI given the features reported in Table 1, including constructive, morphological and heritage-related parameters, as well as of their FDE, which is affected by a generally isolated position within the urban layout.

6. Discussion

The results of this study confirm the potential of the proposed methodology as an innovative and quick-to-apply approach to integrating vulnerability and exposure of buildings and their users within a unique assessment framework. By combining the user distribution over time, the method captures critical spatiotemporal dynamics that influence exposure and vulnerability at the building scale. The following sections will address the key findings from the case study (Section 6.1), implications for policymakers (Section 6.2), and limitations and future work (Section 6.3).

6.1. Key findings from the case study

The case study application highlights the capabilities of the methodology in combining "static" and "dynamic" factors influencing the integrated Vulnerability and Exposure of HUBEs at the building scale. The results point out the critical role of different building intended uses in view of their occupancy intensity and schedules, revealing that user-related aspects could significantly impact the vulnerability profile of buildings with similar physical characteristics.

Residential buildings, typically characterised by a potentially limited and constant number of occupants, exhibit lower and constant exposure and vulnerability levels compared to public functions, as expected. Nevertheless, a relevant variability is observed when user-related components of UEV are integrated with physical components of PV, as shown by dIVE maps (Fig. 13), despite the morphological and constructive homogeneity of the residential buildings. These results reflect the influence of typical daily routines, socio-demographic factors and user familiarity with the environment, which affect exposure and the efficiency of emergency responses even in low-density contexts.

Non-residential functions, particularly those associated with public services or activities open to the public (e.g., recreational, cultural, or healthcare facilities), demonstrate higher and temporally variable IEV values, closely linked to their opening hours. In this sense, public buildings could benefit from the inclusion of UEV in the integrated assessments. Nevertheless, the case study application suggests that monumental buildings and building heritage, where user flows are limited but structural fragilities prevail, vulnerability and exposure could indeed be rapidly investigated by limiting the analysis to PV.

Healthcare facilities, as the hospital located in the historic centre of Bagnacavallo, being classified as "sensitive" buildings, represent a persistent critical point throughout all time intervals. The combination of high user flow, the presence of potentially vulnerable users, and their limited familiarity with the building contributes to identifying it as a significant vulnerability hotspot.

6.2. Advances in literature and implications for policy-makers

This study advances existing literature by introducing a building-

scale methodology for the integrated assessment of vulnerability and exposure in complex HUBEs, where the heterogeneity of building functions makes the inclusion of UEV parameters particularly critical compared to assessments based solely on physical vulnerability (PV). The proposed framework differs from conventional assessment methodologies in flood scenarios, because it focuses on the integrated vulnerability and exposure of buildings and their occupants to hazards, rather than including hazard intensity or probability as a specific assessment factor. This perspective allows the identification of structural and social fragilities that persist regardless of the specific event, providing a flexible and replicable framework for multiple conditions of hazard levels.

By combining PV and UEV, this method captures both "static" physical and functional characteristics of the built environment and the "dynamic" variability of user presence. The inclusion of time-dependent occupancy patterns enables a more realistic representation of urban vulnerability, advancing beyond conventional "static" assessment methodologies (Davis et al., 2023; Ferreira & Santos, 2020). In this sense, key innovations of the proposed approach refer to:

- the combination of exposure and vulnerability components at the building scale in HUBEs, to jointly trace PV parameters, related to the physical elements of the buildings, and UEV parameters, related to the occupants of the buildings, by working at the microscale;
- the structured analysis of the influence of the physical environment versus the human dimension in shaping exposure and vulnerability of buildings and their users. This distinction allows for a comprehensive assessment of building fragility and user dynamics, by using a new comparison indicator, *dIVE*, to map effects in the HUBE scale;
- the revision of previous approaches to include specific parameters in PV and UEV, related to: "static" components, related to the buildings, that are Flood Direction Exposure (*FDE*) [-] and Road Width (*RW*) [-] indexes; and "dynamic" components, related to user vulnerability by adopting use-vulnerability weights, easily associated with use classes (thus depending on groups of building functions).

Furthermore, for the first time at the authors' knowledge, the operational potential of the proposed framework allows for relying on the microscopic analysis of building and user exposure and vulnerability to floods. It enables multi-scalar, informed decision-making and paves the way towards the identification of risk reduction strategies in flood-prone heritage contexts, overcoming current limitations of meso-scale approaches, which still adopt the same "dynamic" approach in temporal analysis (Bernardini et al., 2024).

Decision makers for local authorities and Civil Protection Bodies can then use the results to support the prioritisation of risk reduction strategies, including both structural ones, related to interventions on buildings (mainly to reduce PV), and non-structural ones, related to the management of emergency conditions (mainly to face UEV). Structural interventions could be prioritised by identifying spatial hotspots and matching them with preservation and conservation criteria, while their impacts could be evaluated at different times of the day using UEV data. Non-structural strategies, indeed, can be planned according to both spatial location and critical time intervals, deploying resources where and when IVE peaks. This temporal perspective supports the implementation of time-sensitive emergency plans, enabling decision-makers to anticipate changes in exposure conditions and to focus rescue operations on buildings or areas with critical UEV values. Nevertheless, the results for the case study also suggest a compensatory effect between these PV and UEV: in some cases, high PV is balanced by low UEV, while in others, significant UEV amplifies the risk-affecting conditions associated with low PV values. In particular, building hosting sensitive users (such as elderly individuals, children, or patients) should be prioritised for preparedness and mitigation measures, given their limited ability to self-evacuate and higher dependence on assistance (Hsiao et al., 2021; Lumbroso & Davison, 2018). This "dynamic" prioritisation could also inform real-time emergency alerts, evacuation planning, and temporal management of public functions. Finally, this study contributes to bridging the gap between scientific modelling and policy-oriented decision-making. By translating quantitative indicators into interpretable, spatially explicit outputs, it provides a replicable and scalable framework that fosters evidence-based urban governance. In this context, thanks to the integration of spatial, physical and social dimensions within a single assessment platform, the methodology provides a robust and feasible tool for evidence-based decision-making, supporting both immediate preparedness actions and long-term resilience planning in complex urban environments The approach encourages a shift from reactive emergency response to proactive, time-aware resilience planning, aligning scientific insight with the operational and social needs of historic urban environments.

6.3. Limitations and future work

Despite the promising results and the demonstrated capability of the proposed methodology, it is essential to acknowledge that certain limitations have emerged in its current application.

First, the analysis focused on a single scenario of urban use and occupancy, limiting comparative validation across different spatial configurations and planning scenarios. Although the methodology is developed for scalability and cross-case applicability, it has yet to be tested under varying user densities, functional distributions, and morphological conditions, and should also be extended to other case studies. These variables could significantly influence the methodology's performance and sensitivity, particularly in areas characterised by more complex topographies or historically constrained urban fabrics, where morphological and elevation differences may further affect building exposure and vulnerability patterns.

Second, the temporal resolution adopted in the current implementation, based on a limited number of fixed daily time intervals, facilitated the identification of general trends in exposure and vulnerability. Nevertheless, it failed to capture micro-scale temporal dynamics, such as hourly variations or seasonal fluctuations. Expanding the temporal resolution would enhance modelling of user patterns, particularly in urban areas characterised by high tourist variability or periodic events (Camacho-Caballero et al., 2025; Jaafari et al., 2024; Musolino et al., 2022; Renner et al., 2018).

Third, the estimation of the exposure index relies on typological, standardised occupant load values defined by the Italian fire safety code. While this approach ensures methodological consistency and replicability, it provides conservative results, and thus it could overestimate user density under optimal conditions. Although occupancy trends are generally easy to estimate due to knowledge of opening hours, the transient and heterogeneous nature of users, often unfamiliar with the environment, would require additional efforts to increase model reliability. As a consequence, this approach could reduce the accuracy of exposure assessments with respect to the effective occupancy schedules of the HUBE components, particularly in buildings or functions that generally operate below maximum capacity. Future research should refine occupancy modelling through time-dependent corrective factors, exposure calculations based on net areas, and in-situ surveys from representative case studies. The implementation of specific indices to capture user variability, together with the definition of "what-if" scenarios and storylines simulating alert and evacuation conditions, developed in collaboration with Civil Protection Bodies and local authorities, would further enhance the realism and reliability of the framework, especially in behavioural and emergency response simulations.

Fourth, the current weighting system, based on consolidated standards related to homogeneous ranges and AHP techniques, is developed to ensure transparency and reproducibility (Agliata et al., 2021, 2022; Ashfaq et al., 2025; Bernardini et al., 2024). Nevertheless, in view of possible related bias due to subjectivity, the indicator weighting should

be further investigated, following the criteria of adaptability and reliability in line with the decision-makers' needs (Papathoma-Köhle, 2016). Different directions could be followed in this sense. A sensitivity analysis (which is absent in the current version of the research, but also in most of the previous approaches) would represent a further step to understand how changes in weighting affect outcomes. The group of experts involved in the weighting assignment could be further increased, including local administration and their technicians, and by preferring simple strategies, such as AHP. Indeed, alternative weighting methodologies could be investigated to assess how variations in factor importance affect results, including AHP combination with entropy-based, or fuzzy logic systems (Huang & Feng, 2025; Liu et al., 2020). These approaches would facilitate context-specific calibration of parameters and provide valuable insight into the robustness and replicability of the framework across different case studies.

Finally, the current workflow does not directly consider flood hazard modelling (e.g., flood depth, discharge, or return period), focusing instead on the intrinsic components of vulnerability and exposure. This strategy ensures broader applicability across different contexts. It could be further enhanced by integrating flood dynamics models alongside data or stakeholder needs, allowing for the combined effects of floodwaters spreading in the urban layout with possible damage effects depending on PV features. A similar concept could also be extended to human losses.

Extending the framework to multi-hazard and behavioural modelling would enable the analysis of interactions between physical, social, and operational dimensions (Julià & Ferreira, 2021; Sharifi, 2023). This can support the understanding of how built environments and their users respond under stress conditions, as well as it can contribute to the development of holistic, adaptive, and risk-informed urban planning strategies. In particular, this integration would enhance the capacity to simulate real-time responses and adaptive behaviours, supporting the development of more comprehensive, evidence-based, user-oriented strategies for urban resilience and emergency management, primarily focused on identified critical parts and hot-spots of the urban built environment. Future research should also aim to extend the methodology across different functional, spatial, and planning scenarios, enhancing both temporal resolution and scalability. In this sense, integrating the proposed approach within multi-hazard assessment frameworks, including damage modelling and evacuation simulation, would also enable the representation of behavioural responses, warning protocols, and preparedness levels.

7. Conclusions

This study proposed a methodological framework for the integrated assessment of vulnerability and exposure in Historic Urban Built Environments (HUBEs), addressing the limitations of conventional, hazard-centred approaches. By jointly analysing "static" (physical) and "dynamic" (user-related) components, the methodology reveals spatial and temporal variations in vulnerability that traditional "static" assessments often overlook. The Integrated Vulnerability and Exposure Index (IVE) and its differential form (dIVE) capture how the interaction between structural fragility and user dynamics shapes the overall predisposition of urban assets to potential hazards. This approach moves towards the reshaping of exposure and vulnerability as a context-dependent and time-evolving property of the built environment.

The relevant application to an Italian historic case study results confirm that user-related dynamics play a decisive role in defining vulnerability patterns, particularly within functionally heterogeneous urban contexts. Residential buildings exhibit relatively stable conditions, whereas public, cultural, and service facilities display pronounced temporal fluctuations associated with their activity cycles. Sensitive uses (such as healthcare or educational facilities) consistently emerge as critical hotspots, where high user density, mobility constraints, and the presence of vulnerable individuals amplify exposure and limit emergency response capacity. These findings emphasise the importance of integrating user-oriented parameters with physical attributes to fully capture the multi-dimensional nature of urban exposure and vulnerability.

Beyond its analytical contribution, the framework provides a robust decision-support tool for local authorities and Civil Protection Bodies. By translating complex spatio-temporal data into interpretable indicators, it supports the prioritisation of both structural and non-structural strategies. Structural interventions can be aligned with conservation and safety objectives, while non-structural measures - such as adaptive evacuation planning, "dynamic" management of public functions, or time-sensitive coordination of emergency resources - can be tailored to periods of peak vulnerability. This capacity for time-aware governance strengthens preparedness and operational efficiency, particularly in heritage contexts where physical modifications are constrained.

Finally, the proposed methodology provides a scalable and adaptable foundation for future research, enabling the integration of "dynamic", user-oriented vulnerability assessments within multi-hazard and behavioural frameworks. By isolating intrinsic vulnerability and exposure factors, while allowing refinement through advanced hazard modelling, behavioural simulation, and context-specific weighting systems, it supports evidence-based decision-making and resilience planning in complex HUBEs.

CRediT authorship contribution statement

Gessica Sparvoli: Writing – review & editing, Writing – original draft, Visualization, Software, Methodology, Investigation, Formal analysis, Data curation. **Elena Bosi:** Writing – original draft, Visualization, Software, Resources, Methodology, Investigation, Formal analysis, Data curation. **Gabriele Bernardini:** Writing – review & editing, Writing – original draft, Validation, Methodology, Conceptualization. **Enrico Quagliarini:** Writing – review & editing, Supervision, Project administration, Funding acquisition, Conceptualization, Methodology. **Tiago Miguel Ferreira:** Writing – review & editing, Writing – original draft, Validation, Supervision, Project administration, Methodology, Funding acquisition, Conceptualization.

Declaration of competing interest

The authors declare that they have no known competing financial interests or personal relationships that could have appeared to influence the work reported in this paper.

Appendix A

Fig. A.1, Fig. A.2, Fig. A.3

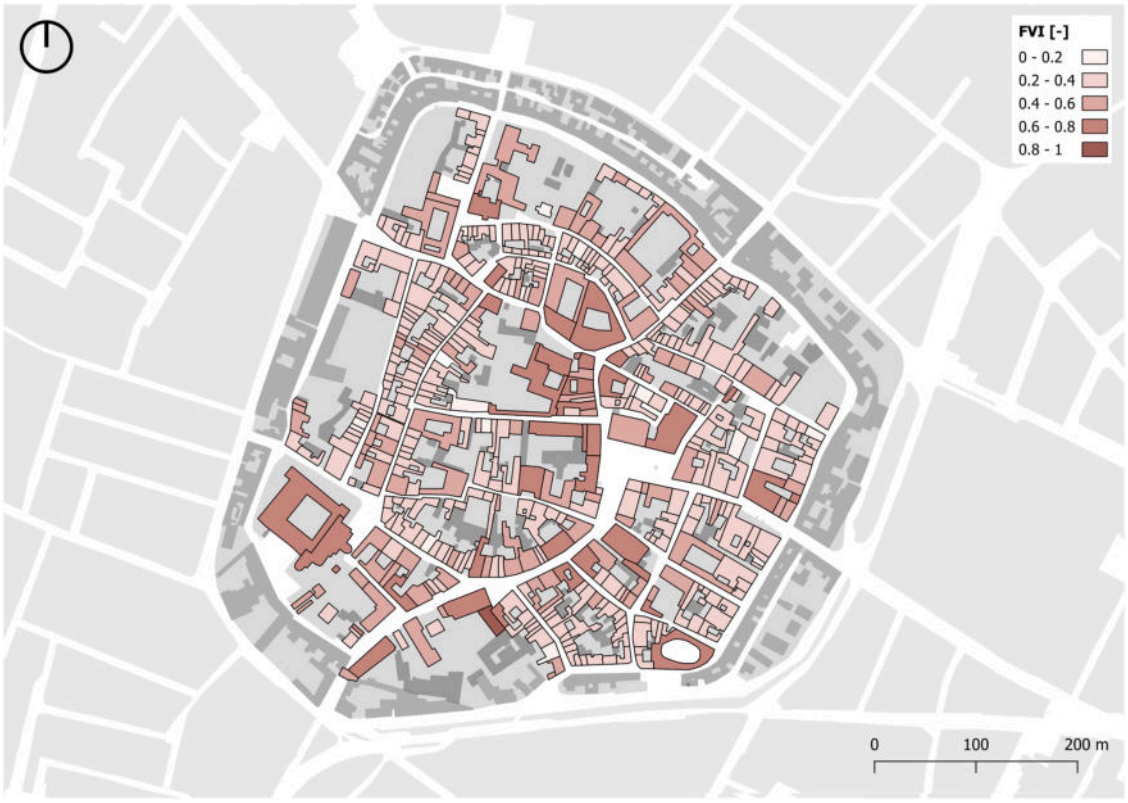

Fig. A.1. Map of Flood Vulnerability Index (FVI).

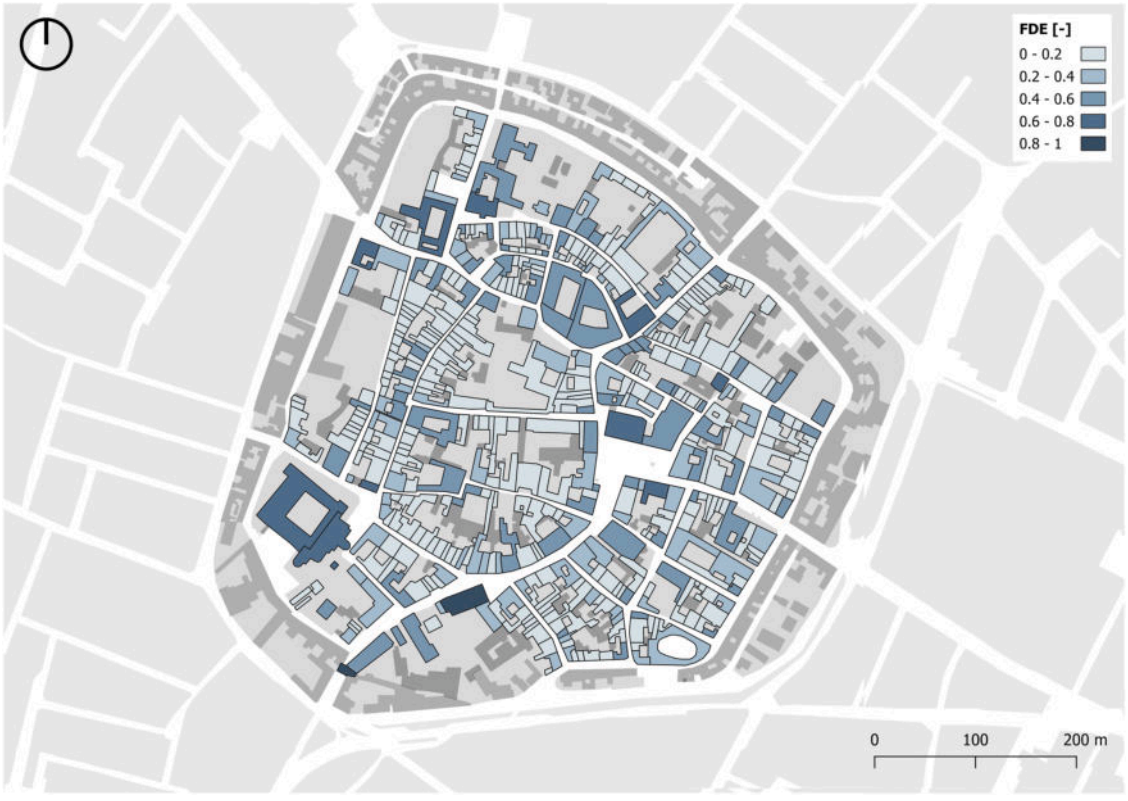

Fig. A.2. Map of Flood Direction Exposure (FDE).

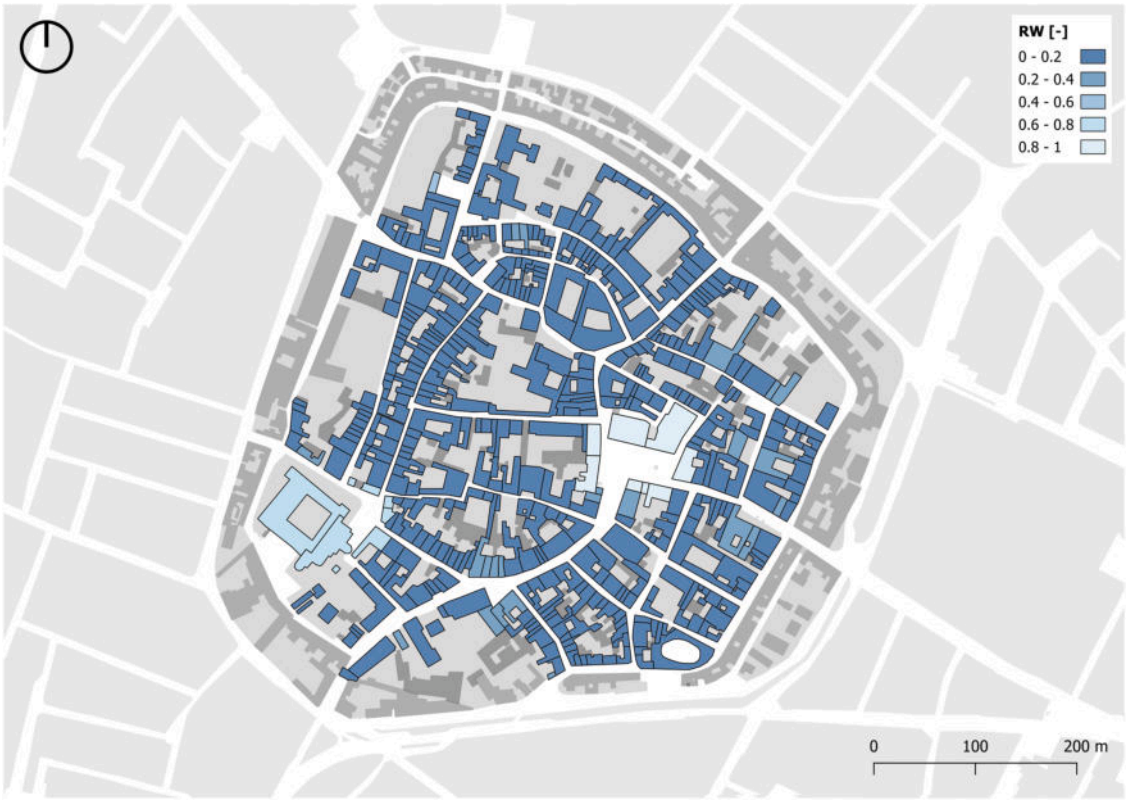

Fig. A.3. Map of Road Width (RW).

Data availability

Data will be made available on request.

References

Abigail, W., Jonathan, G., & Herriet, E. (2018). *The toxic school run, how toxic air is putting children's health in danger*. https://www.unicef.org.uk/publications/the-toxic-school-run/.

Agliata, R., Bortone, A., & Mollo, L. (2021). Indicator-based approach for the assessment of intrinsic physical vulnerability of the built environment to hydro-meteorological hazards: Review of indicators and example of parameters selection for a sample area. *International Journal of Disaster Risk Reduction, 58*, Article 102199. https://doi.org/10.1016/j.ijdrr.2021.102199

Agliata, R., Bortone, A., & Mollo, L. (2022). The impact of the aggregation formula on indicator-based method for the assessment of building susceptibility to hydro-meteorological hazards. *International Journal of Disaster Risk Reduction, 72*, Article 102850. https://doi.org/10.1016/j.ijdrr.2022.102850

Arrighi, C., Rossi, L., Trasforini, E., Rudari, R., Ferraris, L., Brugioni, M., Franceschini, S., & Castelli, F. (2018). Quantification of flood risk mitigation benefits: A building-scale damage assessment through the RASOR platform. *Journal of Environmental Management, 207*, 92–104. https://doi.org/10.1016/j.jenvman.2017.11.017

Arrighi, C., Tanganelli, M., Cristofaro, M. T., Cardinali, V., Marra, A., Castelli, F., & De Stefano, M. (2023). Multi-risk assessment in a historical city. *Natural Hazards, 119* (2), 1041–1072. https://doi.org/10.1007/s11069-021-05125-6

Ashfaq, S., Tufail, M., Niaz, A., Muhammad, S., Alzahrani, H., & Tariq, A. (2025). Flood susceptibility assessment and mapping using GIS-based analytical hierarchy process and frequency ratio models. *Global and Planetary Change, 251*, Article 104831. https://doi.org/10.1016/j.gloplacha.2025.104831

Balaian, S. K., Sanders, B. F., & Abdolhosseini Qomi, M. J. (2024). How urban form impacts flooding. *Nature Communications, 15*(1), 6911. https://doi.org/10.1038/s41467-024-50347-4

Bernabeu-Bautista, Á., Serrano-Estrada, L., & Martí, P. (2023). The role of successful public spaces in historic centres. Insights from social media data. *Cities, 137*, Article 104337. https://doi.org/10.1016/j.cities.2023.104337

Bernardini, G., Ferreira, T. M., Baquedano Julià, P., Ramírez Eudave, R., & Quagliarini, E. (2024). Assessing the spatiotemporal impact of users' exposure and vulnerability to flood risk in urban built environments. *Sustainable Cities and Society, 100*, Article 105043. https://doi.org/10.1016/j.scs.2023.105043

Bernardini, G., Sparvoli, G., Cantatore, E., Bruno, S., Fatiguso, F., Isacco, I., Salvalai, G., & Quagliarini, E. (2025). From single to multi-risk perspective: How heatwaves risk mitigation solutions can reduce terrorist risk in historic outdoor open areas. *Sustainable Cities and Society.* , Article 106412. https://doi.org/10.1016/j.scs.2025.106412

Bernardini, G., Quagliarini, E., D'Orazio, M., & Brocchini, M. (2020). Towards the simulation of flood evacuation in urban scenarios: Experiments to estimate human motion speed in floodwaters. *Safety Science, 123*, Article 104563. https://doi.org/10.1016/j.ssci.2019.104563

Bernardini, G., Romano, G., Soldini, L., & Quagliarini, E. (2021). How urban layout and pedestrian evacuation behaviours can influence flood risk assessment in riverine historic built environments. *Sustainable Cities and Society, 70*, Article 102876. https://doi.org/10.1016/j.scs.2021.102876

Calbi, A.; Susini, G. (1994). *Storia di Bagnacavallo (Vol. I)* (Comune di Bagnacavallo /Edizioni Mediateca (ed.)).

Camacho-Caballero, D., Langemeyer, J., Segura-Barrero, R., Vervoort, G., Barton, D. N., & Villalba, G. (2025). Bridging local and global vulnerabilities for an integrated assessment of nature-based solutions. *Sustainable Cities and Society, 130*, Article 106508. https://doi.org/10.1016/j.scs.2025.106508

Cantatore, M. F. A. (2023). Da placentia a placencia. *Trasformazione della morfologia urbana di Piacenza dall'età tardoantica all'alto medioevo*.

Carminati, E., & Martinelli, G. (2002). Subsidence rates in the Po Plain, northern Italy: The relative impact of natural and anthropogenic causation. *Engineering Geology, 66* (3–4), 241–255. https://doi.org/10.1016/S0013-7952(02)00031-5

Castaldini, D., Marchetti, M., Norini, G., Vandelli, V., & Zuluaga Vélez, M. C. (2019). Geomorphology of the central Po Plain, Northern Italy. *Journal of Maps, 15*(2), 780–787. https://doi.org/10.1080/17445647.2019.1673222

Chen, H., Xu, Z., Liu, Y., Huang, Y., & Yang, F. (2022). Urban flood risk assessment based on dynamic population distribution and fuzzy comprehensive evaluation. *International Journal of Environmental Research and Public Health, 19*(24), Article 16406. https://doi.org/10.3390/ijerph192416406

Chen, Y. (2022). Flood hazard zone mapping incorporating geographic information system (GIS) and multi-criteria analysis (MCA) techniques. *Journal of Hydrology, 612*, Article 128268. https://doi.org/10.1016/j.jhydrol.2022.128268

Cherfaoui, D., & Djelal, N. (2019). Change in use and development of public squares considering daily temporalities. *Articulo – Revue de Sciences Humaines*. https://doi.org/10.4000/articulo.3809

Cremonini, I. (2004). *Analisi, valutazione e riduzione dell'esposizione e della vulnerabilità sismica dei sistemi urbani nei piani urbanistici attuativi. Regione Emilia-Romagna, Direzione generale Programmazione territoriale e sistemi di mobilità, Servizio Riqualificazione urb*.

D'Amico, A., Bernardini, G., Lovreglio, R., & Quagliarini, E. (2023). A non-immersive virtual reality serious game application for flood safety training. *International Journal of Disaster Risk Reduction, 96*, Article 103940. https://doi.org/10.1016/j.ijdrr.2023.103940

da Silva, L. B. L., Humberto, J. S., Alencar, M. H., Ferreira, R. J. P., & de Almeida, A. T. (2020). GIS-based multidimensional decision model for enhancing flood risk prioritization in urban areas. *International Journal of Disaster Risk Reduction, 48*, Article 101582. https://doi.org/10.1016/j.ijdrr.2020.101582

da Silva, L. B. L., Alencar, M. H., & de Almeida, A. T. (2022). A novel spatiotemporal multi-attribute method for assessing flood risks in urban spaces under climate change and demographic scenarios. *Sustainable Cities and Society, 76*(July 2021), Article 103501. https://doi.org/10.1016/j.scs.2021.103501

Dabbeek, J., Crowley, H., Silva, V., & Ozcebe, S. (2025). Impact of population spatiotemporal patterns on earthquake human losses. *International Journal of Disaster Risk Reduction, 122*, Article 105455. https://doi.org/10.1016/j.ijdrr.2025.105455

Daníelsson, J., & Zigrand, J.-P. (2006). On time-scaling of risk and the square-root-of-time rule. *Journal of Banking & Finance, 30*(10), 2701–2713. https://doi.org/10.1016/j.jbankfin.2005.10.002

Davis, L., Larionova, T., Patel, D., Tse, D., Baquedano Juliá, P., Pinto Santos, P., & Ferreira, T. M. (2023). Flood vulnerability and risk assessment of historic urban areas: Vulnerability evaluation, derivation of depth-damage curves and cost–benefit analysis of flood adaptation measures applied to the historic city centre of Tomar, Portugal. *Journal of Flood Risk Management, 16*(3), 1–18. https://doi.org/10.1111/jfr3.12908

Dong, Y., Zhang, G., Hong, W.-C., & Xu, Y. (2010). Consensus models for AHP group decision making under row geometric mean prioritization method. *Decision Support Systems, 49*(3), 281–289. https://doi.org/10.1016/j.dss.2010.03.003

Ellena, M., Breil, M., & Soriani, S. (2020). The heat-health nexus in the urban context: A systematic literature review exploring the socio-economic vulnerabilities and built environment characteristics. *Urban Climate, 34*. https://doi.org/10.1016/j.uclim.2020.100676

EU Floods Directive 2007/60/EC. (2007). https://eur-lex.europa.eu/legal-content/EN/TXT/?uri=celex:32007L0060.

Evans, B., Lam, A., West, C., Ahmadian, R., Djordjević, S., Chen, A., & Pregnolato, M. (2024). A combined stability function to quantify flood risks to pedestrians and vehicle occupants. *Science of The Total Environment, 908*, Article 168237. https://doi.org/10.1016/j.scitotenv.2023.168237

Ferreira, T. M., & Santos, P. P. (2020). An integrated approach for assessing flood risk in historic City centres. *Water, 12*(6), 1648. https://doi.org/10.3390/w12061648

Geoportale - Regione Emilia Romagna, (n.d.). https://geoportale.regione.emilia-romagna.it/download.

Giuliani, F., De Falco, A., & Cutini, V. (2020). The role of urban configuration during disasters. A scenario-based methodology for the post-earthquake emergency management of Italian historic centres. *Safety Science, 127*(February), Article 104700. https://doi.org/10.1016/j.ssci.2020.104700

Goepel, K.D. (2013). *Implementing the analytic hierarchy process as a standard method for multi-criteria decision making in corporate enterprises – a new AHP Excel template with multiple inputs*. https://doi.org/10.13033/isahp.y2013.047.

Goepel, K. D. (2018). Implementation of an online software tool for the analytic hierarchy process (AHP-OS). *International Journal of the Analytic Hierarchy Process, 10*(3). https://doi.org/10.13033/ijahp.v10i3.590

Guidelines for flood risk. https://www.iononrischio.gov.it/it/preparati/alluvione/?utm_source=chatgpt.com#. n.d.

Hamasha, M. M., Ali, H., Hamasha, S., & Ahmed, A. (2022). Ultra-fine transformation of data for normality. *Heliyon, 8*(5), Article e09370. https://doi.org/10.1016/j.heliyon.2022.e09370

He, R., Tiong, R. L. K., Yuan, Y., & Zhang, L. (2024). Enhancing resilience of urban underground space under floods: Current status and future directions. *Tunnelling and Underground Space Technology, 147*, Article 105674. https://doi.org/10.1016/j.tust.2024.105674

Hillier, B., Leaman, A., Stansall, P., & Bedford, M. (1976). Space syntax. *Environment and Planning B: Planning and Design, 3*(2), 147–185. https://doi.org/10.1068/b030147

Holicky, M., & Sykora, M. (2010). *Risk assessment of heritage structures endangered by fluvial floods*. 205–213. https://doi.org/10.2495/FRIAR100181.

Hsiao, C.-C., Sun, M.-C., Chen, A. Y., & Hsu, Y.-T. (2021). Location problems for shelter-in-place deployment: A case study of vertical evacuation upon dam-break floods. *International Journal of Disaster Risk Reduction, 57*. https://doi.org/10.1016/j.ijdrr.2021.102048

Huang, Z., & Feng, C. (2025). Comprehensive evaluation of urban storm flooding resilience by integrating AHP–Entropy weight method and cloud model. *Water, 17*(17), 2576. https://doi.org/10.3390/w17172576

ISPRA. https://www.isprambiente.gov.it/it/istituto-informa/comunicati-stampa/anno-2025.

ISTAT. https://www.istat.it/. n.d.

Jaafari, A., Mafi-Gholami, D., & Yousefi, S. (2024). A spatiotemporal analysis using expert-weighted indicators for assessing social resilience to natural hazards. *Sustainable Cities and Society, 100*, Article 105051. https://doi.org/10.1016/j.scs.2023.105051

Julià, P. B., & Ferreira, T. M. (2021). From single- to multi-hazard vulnerability and risk in historic Urban Areas: A literature review. *Natural Hazards, 108*(1), 93–128. https://doi.org/10.1007/s11069-021-04734-5

Kang, J., Körner, M., Wang, Y., Taubenböck, H., & Zhu, X. X. (2018). Building instance classification using street view images. *ISPRS Journal of Photogrammetry and Remote Sensing, 145*, 44–59. https://doi.org/10.1016/j.isprsjprs.2018.02.006

Kim, J., Park, J., Park, S., & Kang, J. (2024). Enhancing water management and urban flood resilience using Hazard Capacity Factor Design (HCFD) model: Case study of Eco-Delta city, Busan. *Sustainable Cities and Society, 115*, Article 105851. https://doi.org/10.1016/j.scs.2024.105851

Lassandro, P., Zaccaro, S. A., & Di Turi, S. (2024). Mitigation and adaptation strategies for different urban fabrics to face increasingly hot summer days due to climate change. *Sustainability, 16*(5), 2210. https://doi.org/10.3390/su16052210

Li, W., Yu, J., Chen, D., Lin, Y., Dong, R., Zhang, X., He, C., & Fu, H. (2025). Fine-grained building function recognition with street-view images and GIS map data via geometry-aware semi-supervised learning. *International Journal of Applied Earth Observation and Geoinformation, 137*, Article 104386. https://doi.org/10.1016/j.jag.2025.104386

Liu, Y., Eckert, C. M., & Earl, C. (2020). A review of fuzzy AHP methods for decision-making with subjective judgements. *Expert Systems with Applications, 161*, Article 113738. https://doi.org/10.1016/j.eswa.2020.113738

Lumbroso, D., & Davison, M. (2018). Use of an agent-based model and Monte Carlo analysis to estimate the effectiveness of emergency management interventions to reduce loss of life during extreme floods. *Journal of Flood Risk Management, 11*, S419–S433. https://doi.org/10.1111/jfr3.12230

Macintyre, H. L., Heaviside, C., Taylor, J., Picetti, R., Symonds, P., Cai, X.-M., & Vardoulakis, S. (2018). Assessing urban population vulnerability and environmental risks across an urban area during heatwaves – Implications for health protection. *Science of The Total Environment, 610–611*. https://doi.org/10.1016/j.scitotenv.2017.08.062

Malekinezhad, H., Sepehri, M., Pham, Q. B., Hosseini, S. Z., Meshram, S. G., Vojtek, M., & Vojteková, J. (2021). Application of entropy weighting method for urban flood hazard mapping. *Acta Geophysica, 69*(3), 841–854. https://doi.org/10.1007/s11600-021-00586-6

Mao, H., Fan, X., Guan, J., Chen, Y.-C., Su, H., Shi, W., Zhao, Y., Wang, Y., & Xu, C. (2019). Customer attractiveness evaluation and classification of urban commercial centers by crowd intelligence. *Computers in Human Behavior*, 100. https://doi.org/10.1016/j.chb.2018.08.019

Mebarki, A., Valencia, N., Salagnac, J. L., & Barroca, B. (2012). Flood hazards and masonry constructions: A probabilistic framework for damage, risk and resilience at urban scale. *Natural Hazards and Earth System Sciences, 12*(5), 1799–1809. https://doi.org/10.5194/nhess-12-1799-2012

Mignot, E., Li, X., & Dewals, B. (2019). Experimental modelling of urban flooding: A review. *Journal of Hydrology, 568*(November 2018), 334–342. https://doi.org/10.1016/j.jhydrol.2018.11.001

Mileu, N., & Queiròs, M. (2022). Nighttime and daytime population estimation from open data. *Geographia Technica, 17*(2/2022). https://doi.org/10.21163/GT_2022.172.15

Miranda, F. N., & Ferreira, T. M. (2019). A simplified approach for flood vulnerability assessment of historic sites. *Natural Hazards*. https://doi.org/10.1007/s11069-018-03565-1

Montanari, M.; Ridolfi, M.; Zangheri, R. (2004). *Storia dell'Emilia Romagna* (Laterza (ed.)).

Moreira, L. L., de Brito, M. M., & Kobiyama, M. (2021). Review article: A systematic review and future prospects of flood vulnerability indices. *Natural Hazards and Earth System Sciences, 21*(5), 1513–1530. https://doi.org/10.5194/nhess-21-1513-2021

Musolino, G., Ahmadian, R., & Xia, J. (2022). Enhancing pedestrian evacuation routes during flood events. *Natural Hazards*. https://doi.org/10.1007/s11069-022-05251-9

Pacetti, T., Cioli, S., Castelli, G., Bresci, E., Pampaloni, M., Pileggi, T., & Caporali, E. (2022). Planning Nature based solutions against urban pluvial flooding in heritage cities: A spatial multi criteria approach for the city of Florence (Italy). *Journal of Hydrology: Regional Studies, 41*, Article 101081. https://doi.org/10.1016/j.ejrh.2022.101081

Papathoma-Köhle, M. (2016). Vulnerability curves vs. vulnerability indicators: Application of an indicator-based methodology for debris-flow hazards. *Natural Hazards and Earth System Sciences, 16*(8), 1771–1790. https://doi.org/10.5194/nhess-16-1771-2016

Papathoma-Köhle, M., Cristofari, G., Wenk, M., & Fuchs, S. (2019). The importance of indicator weights for vulnerability indices and implications for decision making in disaster management. *International Journal of Disaster Risk Reduction, 36*, Article 101103. https://doi.org/10.1016/j.ijdrr.2019.101103

Papathoma-Köhle, M., Kappes, M., Keiler, M., & Glade, T. (2011). Physical vulnerability assessment for alpine hazards: State of the art and future needs. *Natural Hazards, 58*(2), 645–680. https://doi.org/10.1007/s11069-010-9632-4

Perimetrazione aree allagate eventi 2023-2024, (n.d.). https://servizimoka.regione.emilia-romagna.it/mokaApp/apps/allagam_202305/index.html.

Piano di Emergenza e di Protezione Civile. (2025). https://www.labassaromagna.it/Documenti-e-dati/Documenti-funzionamento-interno/Piano-di-Emergenza-e-di-Protezione-civile-dell-Unione.

Piano di Gestione del Rischio da Alluvione - PGRA. (n.d.). https://ambiente.regione.emilia-romagna.it/it/suolo-bacino/sezioni/piano-di-gestione-del-rischio-alluvioni.

Piano Particolareggiato del Centro Storico - PPCS. (2023). https://www.labassaromagna.it/Documenti-e-dati/Documenti-tecnici-di-supporto/Piano-Particolareggiato-del-Centro-Storico-PPCS.

QGIS. (n.d.). https://qgis.org/.

Quagliarini, E., Bernardini, G., Romano, G., & D'Orazio, M. (2023). Users' vulnerability and exposure in Public Open Spaces (squares): A novel way for accounting them in multi-risk scenarios. *Cities, 133*, Article 104160. https://doi.org/10.1016/j.cities.2022.104160

Renner, K., Schneiderbauer, S., Pruß, F., Kofler, C., Martin, D., & Cockings, S. (2018). Spatio-temporal population modelling as improved exposure information for risk assessments tested in the Autonomous Province of Bolzano. *International Journal of Disaster Risk Reduction, 27*, 470–479. https://doi.org/10.1016/j.ijdrr.2017.11.011

Romão, X., Paupério, E., & Pereira, N. (2016). A framework for the simplified risk analysis of cultural heritage assets. *Journal of Cultural Heritage, 20*, 696–708. https://doi.org/10.1016/j.culher.2016.05.007

La Rosa, D., & Pappalardo, V. (2020). Planning for spatial equity - A performance based approach for sustainable urban drainage systems. *Sustainable Cities and Society, 53* (October 2019), Article 101885. https://doi.org/10.1016/j.scs.2019.101885

Salvalai, G., Blanco Cadena, J. D., Sparvoli, G., Bernardini, G., & Quagliarini, E. (2022). Pedestrian single and multi-risk assessment to SLODs in Urban built environment: A mesoscale approach. *Sustainability, 14*(18), Article 11233. https://doi.org/10.3390/su141811233

Sharifi, A. (2023). Resilience of urban social-ecological-technological systems (SETS): A review. *Sustainable Cities and Society, 99*, Article 104910. https://doi.org/10.1016/j.scs.2023.104910

Stephenson, V., & D'Ayala, D. (2014). A new approach to flood vulnerability assessment for historic buildings in England. *Natural Hazards and Earth System Sciences, 14*(5), 1035–1048. https://doi.org/10.5194/nhess-14-1035-2014

Taramelli, A., Righini, M., Valentini, E., Alfieri, L., Gatti, I., & Gabellani, S. (2022). Building-scale flood loss estimation through vulnerability pattern characterization: Application to an urban flood in Milan, Italy. *Natural Hazards and Earth System Sciences, 22*(11), 3543–3569. https://doi.org/10.5194/nhess-22-3543-2022

Vojinovic, Z., Hammond, M., Golub, D., Hirunsalee, S., Weesakul, S., Meesuk, V., & Abbott, M. (2016). Holistic approach to flood risk assessment in areas with cultural heritage: A practical application in Ayutthaya, Thailand. *Natural Hazards, 81*(1), 589–616. https://doi.org/10.1007/s11069-015-2098-7

Wang, J.-J. (2015). Flood risk maps to cultural heritage: Measures and process. *Journal of Cultural Heritage, 16*(2), 210–220. https://doi.org/10.1016/j.culher.2014.03.002

WebSIT – Sistema Informativo Territoriale, (n.d.). https://websit.labassaromagna.it/WebSIT.aspx?CodProgetto=WS_039UBR_Emerge#.

Wu, W., Zhu, Z., Zheng, X., Liu, S., & Zhang, D. (2025). Pedestrian vulnerability assessment of underground staircases in urban flooding. *Sustainable Cities and Society, 131*, Article 106700. https://doi.org/10.1016/j.scs.2025.106700

Young, A. F., & Jorge Papini, . J.. A.. (2020). How can scenarios on flood disaster risk support urban response? A case study in Campinas Metropolitan Area (São Paulo, Brazil). *Sustainable Cities and Society, 61*, Article 102253. https://doi.org/10.1016/j.scs.2020.102253

Zakariya, K., Harun, N. Z., & Mansor, M. (2014). Spatial characteristics of Urban Square and sociability: A review of the City Square, Melbourne. *Procedia - Social and Behavioral Sciences, 153*, 678–688. https://doi.org/10.1016/j.sbspro.2014.10.099

Zhao, P., Md Ali, Z., & Ahmad, Y. (2023). Developing indicators for sustainable urban regeneration in historic urban areas: Delphi method and Analytic hierarchy process (AHP). *Sustainable Cities and Society, 99*, Article 104990. https://doi.org/10.1016/j.scs.2023.104990